HADLEY CENTRE TECHNICAL NOTE NO. 1

THE SIMULATION OF SST, SEA ICE EXTENTS AND OCEAN HEAT TRANSPORTS IN A VERSION OF THE HADLEY CENTRE COUPLED MODEL WITHOUT FLUX ADJUSTMENTS

by

Chris Gordon, Claire Cooper, Catherine A Senior,
Helene Banks, Jonathan M Gregory, Timothy C Johns,
John F B Mitchell, Richard A Wood

This paper has been submitted to Climate Dynamics

Hadley Centre for Climate Prediction and Research
Meteorological Office
London Road
Bracknell
Berkshire RG12 2SY

NOTE: This paper has not been published. Permission to quote from it should be obtained from the Director of the Hadley Centre.

Abstract

Results are presented from a new version of the Hadley Centre coupled model (HadCM3) that does not require flux adjustments. The model has both an improved atmosphere and ocean component. In particular, the ocean has a 1.25°x1.25° degree horizontal resolution and leads to a considerably improved simulation of ocean heat transports compared to earlier versions with a coarser resolution ocean model. The model does not have any spin up procedure prior to coupling and the simulation has been run for over 400 years starting from observed initial conditions. The SST and sea ice simulation are shown to be stable and realistic. In part, the improved simulation is a consequence of a greater compatibility of the atmosphere and ocean model heat budgets. The atmospheric model surface heat and momentum budget are validated by comparing with climatological ship based estimates. Similarly the ocean model simulation of poleward heat transports is compared with direct ship based observations for a number of sections across the globe. Despite the limitations of the verifying datasets, it is shown that the coupled model is able to reproduce many aspects of the observed heat budget.

1. Introduction

Coupled ocean-atmosphere general circulations models (OAGCMs) have become a valuable tool in attempting to understand and predict climate change (Houghton et al, 1996). One of the major drawbacks of these models has been the large climate drifts that occur when they are used to simulate the current climate. In many models these drifts have been alleviated by the use of flux adjustments (Sausen et al, 1988, Manabe et al, 1991, Johns et al, 1997). Over the past few years a number of developments have been made to the Hadley Centre global coupled model that is used in the investigation of anthropogenic climate change. Recent improvements to both the atmosphere and ocean models have gone a long way towards reducing the model climate drift, and thereby obviated the need for flux adjustment. Other models have also recently demonstrated the ability to produce stable climate simulations without flux adjustments (Barthelet et al, 1998, Boville and Gent, 1998).

This paper describes results from a simulation of pre-industrial climate using the latest version of the Hadley Centre coupled model (HadCM3), which does not use flux adjustments. We concentrate on the analysis of the mean simulation of sea surface temperature (SST), sea ice extents, surface heat and momentum fluxes and ocean heat transports, as these are some of the key climate variables for which, in the past, it has been difficult to obtain a realistic and stable simulation.

It is important to verify that the model realises a stable climate for sound physical reasons with the correct balance of heating terms. Hence we also concentrate on the validation of both the atmospheric model simulation of surface heat fluxes and the ocean model simulation of heat transports. The fresh water budget and the ocean salinity simulation will be discussed in detail in a separate paper. The lack of salinity drifts are equally important in maintaining a stable climate simulation and, as discussed briefly in a later section, the salinity drifts in the model over 400 years do not lead to major changes in the ocean circulation.

Section 2 discusses climate drift in coupled models and provides the framework for the structure of the rest of the paper. In Section 3 the various components of the coupled

model are described. Section 4 outlines the initialisation of the model and the convergence of the coupled model state. The simulation of SST and sea ice extents in the coupled model are discussed in Section 5. Section 6 considers the surface fluxes of heat and momentum from a simulation of the atmospheric model using observed SSTs. These are compared with estimates of these fluxes from climatologies based primarily on ship observations. The ocean heat transports in the model are discussed in Section 7 and, finally, the results are summarised in Section 8.

2. Climate Drift in Coupled Models

The atmosphere and ocean interact via the interface at the sea surface and the SST and sea ice extents are therefore crucial predictands in a coupled model simulation. The simulation of ocean temperatures and sea ice extents also depends critically on ocean heat transports. In any ocean region, in the long term annual mean, the net surface heat exchange must be balanced by the ocean advection of heat into (or out of) the region. In the zonal average this is expressed by the simplified equation for the depth and zonally averaged ocean potential temperature:

$$\rho_0 C_p H \frac{\partial \langle \theta \rangle}{\partial t} + \frac{1}{a \cos\phi} \frac{\partial}{\partial \phi} (F_\theta) = Q_0$$

$$F_\theta = \rho_0 C_p H \langle v\theta \rangle \cos\phi \qquad (1)$$

where $< >$ denotes a zonal and depth average, Q_0 is the zonal mean heating at the surface, F_θ is the flux of heat across the latitude ϕ and H the ocean depth. Other variables are standard notation. Diffusion effects have been ignored in (1) since in most regions they are not a major contribution to the model zonal mean heat budget (see fig.17). It follows from (1) that there will be a net drift in the depth averaged zonal mean potential temperature (i.e. $\partial<\theta>/\partial t \neq 0$) if the ocean meridional advection and net surface heating terms do not balance. It is not a simple matter to relate the vertically integrated temperature changes to SST changes, equation (1) being only applicable to the vertical mean temperature, and within the vertical column there may be compensating temperature drifts. Equation (1) does, however, provide a very basic framework for discussing climate drift in a coupled model.

The equilibrium ocean heat transports implied by the atmospheric model surface fluxes, when the atmospheric model is integrated with observed SSTs, can be easily calculated by the meridional integration of the right hand side in equation (1). This calculation determines the ocean heat transports required to balance the surface exchanges. This estimate can then be compared with the same calculation using both climatological flux estimates and direct ocean observations.

The heat transports can also be calculated from the ocean model, when integrated with climatological surface forcing (i.e. a direct calculation of the $<v\theta>$ term in (1)). Making this estimate is not straight-forward in the ocean only case, as in addition to the climatological surface heat flux, a feedback term on SST is also required in ocean

only simulations (e.g. a Haney (1971) type forcing term or specified atmosphere winds, air temperatures etc.), and the extent to which this relaxation term determines the ocean heat transports is not clear. Comparisons between 'ocean-only' and the fully coupled simulations described below have shown the former to be of limited use in understanding the behaviour of the full coupled system.

It is apparent that if the ocean heat transports implied by the atmospheric model are significantly different to the actual ocean model heat transports, then the coupled model ocean temperatures must drift to enable a new balance to be established. If a stable equilibrium exists then the SST and sea ice extents must drift in such a way as to bring the model implied heat transports to be in balance with the ocean heat transports. (In this paper the terminology 'implied' heat transports will be used for transports determined from the integration of air sea fluxes and 'actual' heat transports those determined either from direct ocean observations or from the calculation of the temperature advection term in the ocean model.) Weaver and Hughes (1996) demonstrated that in a model with climate drift a 'minimum' flux adjustment could be applied which simply ensured the flux balance discussed above in a zonal mean sense. Recently Boville and Gent (1998) have, in part, attributed their success in obtaining a realistic un-flux adjusted coupled simulation to the compatibility of the actual and implied heat fluxes (Bryan, 1998).

Earlier versions of the Hadley Centre coupled model ('UKTR' and 'HadCM2'), which required flux adjustment, certainly showed an imbalance between the implied and actual ocean heat transports. In these earlier versions, SSTs were constrained to be close to reality by application of a flux adjustment in the surface heating term. Fig.1 shows the ocean heat transport from two coupled integrations with the earlier versions of the model. Details of HadCM2 can be found in Johns et al (1997) and UKTR in Murphy (1995). Both the implied heat transports calculated from the atmospheric model surface fluxes and the actual ocean heat transports from the ocean model are shown in fig.1. For comparison, ocean heat transport estimates using the Da Silva et al (1994) flux climatology (hereafter referred to as DS) are also included and, following DS, we assume a transport of 0.1 PW at 65°N. The calculation based on the AGCM fluxes for both model versions is in reasonable agreement with the climatology, especially in the northern hemisphere. The differences in the southern hemisphere will be discussed further in Section 6. The figure also clearly shows that the ocean models used in HadCM2 and UKTR, when integrated in flux adjusted mode, underestimate the ocean heat transports by nearly a factor of two. The flux adjustment term essentially makes up the difference. When the HadCM2 model is integrated without flux adjustments (Gregory and Mitchell, 1997) there is a large SST drift as the coupled model attempts to reach a balanced state.

The above points to the fact that a realistic simulation of both the surface heat fluxes and the ocean heat transports is necessary to reduce climate drift in the surface temperature and sea ice simulation. It is therefore important to validate the heat budget in both component models rather than simply to validate the coupled model SST and sea ice simulation. An initial validation will be presented here for HadCM3. Experience with the un-flux adjusted HadCM3 model has also shown that, away from the equator and strong current regions, the seasonal simulation of SST is strongly

dependent on the surface fluxes. This dependence is in agreement with the observations (Gill and Niiler, 1973).

3. Model Description

3.1 The Atmospheric Component

The atmospheric model used is the HadAM3 version of the UKMO unified forecast and climate model run with a horizontal grid spacing of 2.5° x 3.75° and 19 vertical levels using a hybrid vertical co-ordinate. The timestep is 30 minutes. The performance of this model version in a simulation forced by observed SSTs is described in Pope et al (1998).

Some of the major changes in this model over the previous version used in coupled simulations (Johns et al, 1997) are now described.

i) A new radiation scheme has been included which has 6 (8) spectral bands in the shortwave (longwave) and represents the effects of minor trace gases as well as CO2, H2O and O3. (Edwards and Slingo, 1996). A parametrization of a simple background aerosol climatology (Cusack et al, 1998) is also included.

ii) The convection scheme has been improved by adding a parametrization of the direct impact of convection on momentum (Gregory et al. 1997).

iii) A new land surface scheme (Cox et al. 1998) includes the representation of the freezing and melting of soil moisture and the formulation of evaporation includes the dependence of stomatal resistance on temperature, vapour pressure and CO2.

iv) A parametrization of orographic drag (Milton and Wilson, 1996) and a new gravity wave drag scheme including anisotropy of orography, high drag states and flow blocking, and trapped lee waves have been included (Gregory et al, 1998).

v) The partitioning of mixed phase clouds into ice and water has been changed from 0 to -15 C to 0 to -9 C (Gregory and Morris, 1996) based on evidence from observational data (Moss and Johnson, 1994). A parametrization of the effective radius of cloud droplets as a function of cloud water content and droplet number concentration is also included (Martin et al, 1994). Several parameters in the layer cloud scheme (Smith, 1990) have been altered. Cloud cover forms when the standard deviation of the distribution of total water content in a grid box goes above a critical relative humidity (RHcrit). RHcrit is a constant value at each level of the model. In HadCM3 this has been changed from 0.85 to 0.7 to improve the top of the atmosphere (TOA) radiation balance. The equation for liquid precipitation includes a threshold value of the total water content, C_w, below which water does not precipitate. The value of this threshold is different over land and ocean to represent the different amounts of cloud condensation nuclei. In HadCM3, these values were reduced from 8 x 10^{-4} to 2 x 10^{-4} over land and from 2 x 10^{-4} to 0.5 x 10^{-4} over sea. In combination, these changes improved the net TOA radiative fluxes, especially over northern mid-latitude oceans.

vi) There were some significant revisions to boundary layer mixing; most importantly the removal of a non-local mixing scheme (Smith, 1993), the inclusion of which was found to degrade the transport and sink of aerosols.

In addition to these major model improvements, there have been a number of minor changes. These are documented in Pope et. al (1998)

3.2 The Ocean Component

The ocean model has been specifically developed over a number of years for use in coupled climate simulations. The version used in the simulation described below is substantially different to that previously employed in simulations with the Hadley Centre coupled climate model. The basic model, with a 2.5°x3.75° horizontal resolution ocean component, is described in Johns et al (1997). Here the modifications made in the current version will be focused upon.

The ocean component is a 20 level version of the Cox (1984) model on a 1.25°x1.25° latitude-longitude grid. There are six ocean grid boxes to each atmosphere model grid box and each high latitude ocean grid box can have partial sea ice cover. The vertical levels are distributed to provide enhanced resolution near to the ocean surface and are the same as those in the previous coarser horizontal resolution version of the model (Johns et al, 1997).

Horizontal mixing of tracers uses a version of the Gent and McWilliams (GM) (1990) adiabatic diffusion. Earlier experiments with the 1.25° ocean model showed that it is not appropriate to set a globally constant thickness diffusion coefficient. This was because in order to maintain both the sharp horizontal density gradients associated with the North Atlantic Current and Kuroshio extension and, at the same time, simulate significant eddy fluxes in the Antarctic Circumpolar Current, different thickness diffusion coefficients are required (Wright, 1997). In the model described here, the formulation of Visbeck et al (1997) is therefore used in which the thickness diffusion coefficient is determined locally. The numerical implementation of Griffies (1997) is also employed, as this leads to a considerable reduction in grid point noise by improving the representation of the along isopycnal diffusion. There is no explicit horizontal tracer diffusion in the model. The along isopycnal diffusion coefficient is 1000 m^2s^{-1} and does not vary with depth. The coefficient of horizontal momentum viscosity is formulated as $A_M=A_1+A_2\cos(\text{latitude})$ with $A_1=A_2=3000$ m^2s^{-1}. The latitude dependence of A_M is included to prevent numerical instability at high latitudes as the grid lines converge.

The near surface vertical mixing is parametrized by a hybrid approach in which the mixing of tracers is carried out via a Kraus-Turner mixed layer sub-model (Kraus and Turner, 1967, Gordon and Bottomley, 1985) and mixing of momentum via a K-Theory scheme (Pacanowski and Philander, 1981). The convective adjustment is modified in the region of the Denmark Straits and Iceland-Scotland Ridge to better represent the down slope mixing of the overflow water. The overflow water, rather than convectively mixing throughout the vertical column, is allowed to find its level of neutral buoyancy. The scheme is based on that used by Roether et al (1994).

There is also a parametrization of the outflow of water from the Mediterranean in which water is partially mixed across the Strait of Gibraltar. The sea ice model, which is the same as that used in HadCM2, uses a simple thermodynamic scheme and contains parametrizations of ice drift and leads (Cattle and Crossley, 1995).

3.3 Coastlines

Although the ocean model has a 1.25°x1.25° horizontal grid, for ease of coupling the coastline of the coupled model is that of the atmospheric model 2.5°x3.75° grid. This means that there is only a very coarse representation of the channels between the Pacific and Indian Oceans in the Indonesian through-flow region. In reality the major gap for barotropic flow from the Pacific to the Indian ocean is between Papua New Guinea (PNG) and the Indonesian islands, with flow between Australia and PNG blocked due to shallow topography. Because of the coarse grid coastline, flow occurs through an unrealistic gap between Indonesia and Asia in the original setup of the model. In addition, the minimum water depth of 140m assumed in the model permits too much throughflow. To compensate for the coarse grid, barotropic flow is therefore only allowed in the model between PNG and Indonesia.

3.4 Atmosphere-Ocean Coupling

The models are coupled once per day. The atmospheric model is run with fixed SSTs through the day and the various forcing fluxes are accumulated each atmospheric model timestep. At the end of the day these fluxes are passed to the ocean model which is then integrated forwards in time. The updated SSTs and sea ice extents are then passed back to the atmospheric model. As there are six ocean grid points to every atmospheric grid point interpolation and/or averaging is used to transfer fields between the two grids (see Appendix for details).

3.5 Water conservation

The rigid lid in the ocean model means that the fresh water flux at the ocean surface does not lead to changes in the volume of water in the column. In order to close the global salinity budget the surface salinity boundary condition assumes a constant surface salinity in the ocean of S_0=35 parts per thousand (ppt). Using this constant value means there is no drift in global mean salinity when there is no net water flux, but the local effect of surface fluxes will be exaggerated in regions where $S<S_0$, and under-represented when $S>S_0$.

River runoff is included in the model using predefined river catchments. The runoff enters the ocean at coastal outflow points that are defined on the ocean model grid. There is no explicit river transport in the model, so runoff is transported instantaneously to the ocean. A small amount of model rainfall runs into internal drainage basins and a small term, equivalent to 0.01 $mmday^{-1}$, is applied uniformly over the ocean to allow for this. Even with river runoff included, the area-average water flux in HadCM3 coupled model is not zero. Most of the imbalance, equivalent to a loss of 7.3 $mm\ y^{-1}$ of water averaged over the ocean and a salinity drift of 0.1 PSU in 1000 years, comes from the accumulation of snow on the Antarctic and Greenland ice-sheets, 80% on the former. (These rates compare fairly well with those summarised by Warrick et al, 1996 and with other coupled models such as Russell et al, 1995.) In the real world, fresh water is returned to the ocean by the calving of icebergs, a process not represented in the model. The mass balance of the ice-sheets is not well known so

we therefore assume that accumulation should balance calving for each ice-sheet, and apply an appropriate water flux uniformly over the areas of the adjacent oceans where icebergs occur (Harvey, 1985; Bigg et al, 1996). Of course, the meltwater of the icebergs should not really be uniformly distributed, but the model is not noticeably sensitive to the distribution and the current state of observations and modelling does not justify any more elaborate treatment of this relatively small term. The largest local values of the iceberg term are about 0.15 mm day^{-1}.

Over the North Atlantic iceberg region, these additional terms are about 5% of the size of P-E. In Baffin Bay and much of the Arctic, they are between 10% and 20% and are also above 10% in limited areas around Antarctica, and in small regions near the coast above 20%. Over the majority of the world ocean, they are less than 1% of the size of P-E.

Even if the global-average salinity is constant, a poor simulation of the precipitation and/or evaporation over an individual basin will lead to a local salinity drift in that basin, which will only eventually be checked, perhaps when it has reached an unrealistic value, by exchange with other basins. Poor simulation of surface water fluxes can be more serious than for heat fluxes, because there is no feedback on the fluxes from the salinity drift as there is from temperature. The problem is particularly acute for small isolated basins, such as the Caspian Sea, and others in the model, such as the Baltic, where there is no mixing across the straits which connect them to the world ocean. In these latter cases, the model would be improved by including exchange across the straits (as done, for instance, by Russell et al, 1995). In HadCM3, the salinity at every point is constrained to remain within the limits of 0 and 40 ppt. Some isolated basins reach these limits; keeping them there implies a small non-conservation of water amounting to 0.2 mm y^{-1} averaged over the ocean.

The above issues associated with water conservation and its effects on the salinity drifts in the model were masked in earlier model versions by the use of salinity flux adjustment terms.

4. Coupled Model Initialisation and Convergence

The coupled model was initialised with an atmospheric model state appropriate to mid-September and ocean temperatures and salinities were specified from the Levitus (1994) mean climatology for the month of September. Ocean currents were zero at the initial time. The coupled model simulation was integrated for over 400 years and most of the results that follow in the subsequent sections show fields meaned over the years 81 – 120 and years
361 – 400. It is noteworthy that no prior stand-alone ocean spin-up of the atmosphere and ocean/sea ice models is needed to achieve a balanced initialised state for use in the coupled model.

The model being described here has been developed for use in climate change predictions. It is not crucial that the system is in equilibrium in order to perform such experiments. However the drift due to lack of equilibrium should ideally be much less than the perturbation signal. The timeseries of global mean SST anomaly and top of the atmosphere (TOA) radiative heat flux are shown in fig.2. The SST anomaly is defined as the difference between the model SST and the GISST2.2 values (Rayner et

al, 1996). The trace gas concentrations used in the model are pre-industrial so we expect the model to be approximately 0.3°C colder than the present day GISST temperatures (Houghton et al, 1996). The global SST in the coupled model remains within 0.3°C of climatology over the 400 years of the simulation and there is little sign of a long term systematic drift. There is considerable interannual and interdecadal variability evident in the timeseries. The major characteristics of the geographical pattern of simulated SST are also very stable after the first few decades (to be discussed in the next section). The TOA flux is also generally less than 0.5 Wm^{-2}. Over most of the latter part of the run it is negative, indicating a net cooling of the climate system.

The temperature and salinity drifts below the ocean surface are illustrated in figs.3a and b. In the upper 1000m for the first 50 years of the simulation there is considerable drift in temperatures away from the initial Levitus (1994) state. After this time the drift at these depths becomes considerably smaller with maximum temperature differences 0.5°C too warm at 200m in the zonal mean. In the deep ocean there is a slow cooling which will have a very long equilibration timescale. The timeseries of global volume weighted temperature in fig.3c shows there is a net cooling trend of 0.02°C per century. This cooling trend is consistent with the net heat loss indicated by the TOA flux in fig.2.

The corresponding drift in salinity is shown in fig.3b. After 400 years the depth distribution of the salinity drift shows an increase below 1000m and a freshening above this depth. Over the 400 years of the integration the global average surface salinity freshens by nearly 1 $^{0}/_{00}$, although 50% of this drift occurs in the first 100 years. North Atlantic salinity drifts are particularly important because of their potential impact on the thermohaline overturning circulation. In the North Atlantic the surface salinity freshens by approximately 0.2 $^{0}/_{00}$ over the 400 years of the integration, whereas at 500m there is an increase in salinity of 0.6 $^{0}/_{00}$ over this same period. It will be shown later that the overturning cell in the North Atlantic is stable throughout the integration, demonstrating the relatively small impact of these salinity drifts on the circulation.

Finally, the timeseries of global mean sea ice area and volume are shown in figs.4a and 4b. The ice area (fig.4a) reaches a stable extent in the first few years of the simulation. The ice volume (fig.4b) is also stable but it takes a longer time to reach its long term value. In the first 30 years of the simulation there is a net increase in ice volume indicating an increase in the ice thickness away from its initial value (which was specified from a previous coupled simulation). A comparison with observations of the geographical distribution of sea ice in the model simulation is made in Section 5.

Overall we see that after 400 years, the global mean upper ocean fields have reached a stage of relatively small drift. This capability to start from the observed ocean state (Levitus, 1994) and to maintain this without large drifts over 400 years is a notable success of the model, particularly as no spin-up is required to precondition the coupled model. How much of the cooling in the deep ocean is a consequence of the pre-industrial trace gas concentrations used has not been established. Since a climatology of ocean conditions in pre-industrial times is not available, only modelling experiments will be able to determine this.

5. Simulation of the Sea Surface Temperature and Sea Ice Extents

The SST and sea ice extents, both in reality and in the coupled model, are the central variables through which the atmosphere/ocean/ice coupling takes place. A realistic simulation of these variables is of prime importance in determining the usefulness of the coupled model for climate simulations.

5.1 Sea Surface Temperature

The simulation of annual mean SST is shown in fig.5a averaged over the years 361 - 400. For comparison the same field from the GISST2.2 observed climatology is shown in fig.5b. All of the major observed features in the SST field are reproduced. In particular, the model is able to maintain the sharp horizontal gradients in SST associated with the major ocean currents such as the North Atlantic Current (NAC), Kuroshio and the Antarctic Circumpolar Current (ACC). In making this comparison it should be kept in mind that the GISST2.2 SST dataset is gridded in one degree boxes, and the horizontal SST gradients associated with the major surface currents are considerably sharper than the gradients in the smoothed data. These gradients are maintained in the HadCM3 simulation because of the 1.25° resolution in the ocean model whereas, in earlier un-flux adjusted versions of the coupled model, with a low resolution ocean, these gradients were largely absent. Of course, in flux adjusted models the gradients are artificially maintained by the flux adjustment terms.

There are some notable differences between the model and observed SSTs. The model equatorial central east Pacific is too cold, whereas south of the equator the model is too warm in the eastern tropical Pacific and Atlantic. This is to be expected from the lack of simulated stratocumulus cloud in the atmospheric model which will be discussed in Section 6. The region off the Californian coast is also too warm, probably for the same reasons. The too cold equatorial SSTs are consistent with the excessive equatorial easterlies simulated in the atmosphere-only simulation described later.

These features are better illustrated in the differences between the model SSTs and the GISST climatology of SST as shown in figs.6a and 6b for the time periods covered by the years 81-120 and 361-400. Over most of the ocean the coupled model after 400 years is simulating the SSTs to within 2°C of their observed values. There are, however, some notable regions where the differences are considerably larger than 2°C. A comparison of the SST difference fields for the two time periods shows the pattern is very stable, with the fields being similar in figs.6a and 6b. One notable exception is the greater cooling in the North Atlantic in the later period.

The major systematic error throughout the simulation is the cooling in the North Pacific, where the SSTs are too cold by more than 2°C over a large region. This cooling establishes itself in the first decade of the coupled simulation and its pattern and magnitude remain essentially constant throughout the integration. Analysis of the cooling has pointed most strongly to the poor simulation of surface heat fluxes in this region, combined with the very shallow summer-time mixed layer depths occurring in the North Pacific (in the model and in reality). There is also a local maxima in the cooling in the region of the Kuroshio, which separates from the coast too far south in the model. As the Kuroshio and its extension are associated with high horizontal SST gradients, shifts in their position lead to large local SST errors.

Other than some large local errors associated with shifts in high gradient regions, the North Atlantic is reasonably well represented by the coupled model. The tracking of the North Atlantic current shows to some extent the northward turn in the isotherms to the east of the Grand Banks but this is considerably underestimated compared to reality, especially in the later time period (see figs.5a, 5b and 6b).

The final major error is the warming in the Southern Ocean. Analysis of this drift suggests it is a consequence of a number of complex processes involving the ocean, atmosphere and sea ice models. Excessive surface short wave fluxes, associated with too little cloud in this region, contribute to the warming, as does the seasonal mixing of the surface waters with the deeper and warmer Circumpolar Deep Water (CDW) and the ocean to sea ice heat exchange also plays a part. The peak SST errors in the Southern Ocean are in regions of tight SST gradient and are associated with the incorrect positioning of these gradients (compare the SST fields in figs.5a and 5b). These are also recognised as regions of strong topographic steering of the ACC, and the peak SST errors may well be associated with the incorrect steering of the current in the model. A parallel simulation using an ocean model with 40 vertical levels (the version described here has 20 levels) indeed led to some reduction in the peak errors in the Southern Ocean. In the 40 level model the near bottom resolution was doubled leading to a better representation of topographic steering.

One region of particular note is immediately to the south of the Cape of Good Hope in Southern Africa where there is a significant SST error in figs.6a and 6b. This region is known to be high in eddy activity and it has been suggested that there is a substantial eddy heat flux through this area (Thompson et al, 1997).

The overall SST error pattern described above is similar in many aspects to that found in both the NCAR CSM1 (Boville and Gent, 1998) and ARPEGE T42/OPAICE (Barthelet et al, 1998) un-flux adjusted coupled models. The similarity between the models suggests that the regions described above may be difficult to simulate because of the physical processes governing the SST in these areas. Overall there is a vast improvement in the SST simulation compared to the earlier un-flux adjusted version of the model (HadCM2) with a low resolution ocean component (Gregory and Mitchell, 1997).

5.2 Sea Ice

Because of the importance of the ice-albedo feedback in climate change, a realistic simulation of sea ice distributions is of critical importance in the coupled model. Timeseries of sea ice area and volume for both hemispheres throughout the coupled simulation are shown in figs.7 and 8. The observed SSM/I (Special Sensor Microwave Imager, NSIDC, 1989) maximum and minimum extents are also marked on the figures. In the Arctic the sea ice extents are overestimated at the maxima when compared to the SSM/I data (fig.7a). The reason for these discrepancies can be understood by looking at the modelled geographical distribution of sea ice. Fig.9a shows the simulated annual mean ice concentrations for the northern hemisphere for years 361 - 400. The satellite estimates from SSM/I are also shown in fig.9b for comparison. It can be seen by comparing figures 9a and 9b, and the seasonal cycle of northern hemisphere ice area (fig.11a), that the winter ice extends too far into the North Pacific and the Barents Sea remains ice covered throughout the year. These contribute to the

overestimation of the ice extent maxima. The northern hemisphere ice volume (fig.7b) initially increases and then stabilises after about 30 years.

The northern hemisphere sea ice simulation is much improved over that obtained with un-flux adjusted earlier versions of the Hadley Centre model which employed a low resolution ocean component. In these earlier versions the ice extents were too extensive, reaching south of Iceland in winter. One of the major impacts of using the 1.25°x1.25° ocean model is a much improved simulation of the North Atlantic Current which advects warmer water into the Norwegian Sea and therefore reduces ice cover in this region. Once this warmer water has entered the basin it should, in reality, flow northwards in the Norwegian Current and then split, one component heading northwards as the West Spitsbergen current, another flowing eastwards into the Barents Sea (Pfirman et al, 1994). In the model almost the entire flow is northwards, with very little of this water getting onto the continental shelf. This failure is partly due to the models lack of Svalbard as an island. Sensitivity studies have shown that including the island improves the simulation in the region. As already described, without the warm North Atlantic water reaching the Barents Sea, sea ice is too extensive in this region.

The southern hemisphere ice extents are simulated well compared to climatology, both in the seasonal variation (fig.8a and 11b) and in the mean distribution (fig.10a and 10b). The mean seasonal cycle depicted in fig.11b shows the southern hemisphere wintertime sea ice extents to be too large in the model. The Southern Ocean warming noted earlier in the section does not significantly affect the ice distribution as most of the warming is in summer when the ice extents are close to the coast of Antarctica. There is an adjustment time of around 100 years over which the Antarctic sea ice volume increases towards its long term stable value (fig.8b).

It is important to establish that we have obtained a good simulation of SST and sea ice for the right reasons, and not because of fortuitous cancellation of errors in surface fluxes and ocean heat transports. The following two sections therefore consider the validation of the heat budget in the coupled model.

6. Validation of the Surface Fluxes simulated by the Atmospheric Model

In an atmospheric model, even when the SSTs are specified at their observed values, the calculation of the surface fluxes of momentum (i.e. wind stress), heat and fresh water depends upon a range of simulated model variables including low level winds, air temperatures and humidities, as well as the cloud cover throughout the atmospheric column. These surface fluxes have been variables difficult to simulate realistically in climate and numerical weather prediction models (White, 1996). It is these fluxes which constitute the forcing at the ocean surface in the coupled model and it is therefore important that they are accurately represented. The degree of accuracy required depends upon the sensitivity of the ocean simulation to the various forcings. Considerable work has been done to investigate this ocean sensitivity to wind stress forcing in the tropics (Fevrier et al, 1998) but little has been done over the global oceans.

We consider the mean surface fluxes from a 'stand alone' integration of the atmospheric component of the coupled model for the 10 year period 1979 to 1988.

The SSTs for this experiment were those used in the first Atmospheric Model Intercomparison Project (AMIP-Gates, 1992) and in the remainder of this paper this simulation will be referred to as 'the AMIP simulation'. We concentrate on the fluxes from this atmosphere simulation, rather than those of the coupled simulation, in order to help isolate systematic errors in the component models of the coupled system. Brief comparisons will also be made with coupled model surface fluxes.

This atmospheric model version is identical to that used in the coupled simulation apart from the specification of atmospheric trace gases. The AMIP simulation uses trace gas concentrations appropriate to the 1979 to 1988 period, whereas the coupled model uses pre-industrial values. The simulation of the atmospheric fields in the AMIP simulation is described in Pope et al (1998).

Although our primary interest concerns the surface heat budget we will also attempt to validate the surface wind stress as this is clearly an important forcing function for the ocean. The freshwater budget will be validated in a separate paper. The surface wind stress fields from the model are compared with the climatologies of Hellerman and Rosenstein (HR) (1983) and Josey et al (1996). The surface heat fluxes are compared with the climatological estimates of DS. The validation of the surface fluxes simulated by the atmospheric component of the coupled model is limited by the large uncertainties in the climatological estimates of these fluxes. Throughout the discussion that follows we will concentrate on estimates of the annual mean fluxes simply for clarity and brevity of presentation. These are also the fields that are of most relevance to the long term climate drift in the model. However, we also note that the seasonal evolution of SST is also crucially dependent on the surface flux simulation.

6.1 The surface wind stress

The annual mean surface wind stress from the AMIP simulation is shown in fig.12a and the climatology of HR is shown for comparison in fig.12b. Overall the patterns of wind stress are well simulated. The trade wind regions have higher stresses in HR but this difference is probably within the uncertainty in the climatological estimates. Fig.12c shows the equivalent stress fields from the more recent estimates of Josey et al (1996), and the model is in better agreement with this climatology in the trade wind regions of both hemispheres.

Major differences occur in the Southern Ocean where the model stresses are considerably larger than either climatology although very little data is available in this region. Comparison of low level model winds with equivalent fields from the ECMWF re-analysis climatology (ERA, Gibson et al, 1997) show a good agreement between the climate model and analysis fields in the Southern Ocean although, of course, the ERA will be largely unconstrained in this region and the analysis may reflect systematic errors in the ECMWF model similar to those in climate simulation described here. Further data studies are required to be able properly to validate the model in this region.

There are also significant differences between the model and climatology in the North Atlantic where the simulated stresses in the westerlies are too weak. This is associated with a general high pressure bias at high latitudes, leading to too weak surface pressure gradients in mid-latitudes (see Pope et al, 1998 for details).

In the equatorial regions the Hellerman stresses are known to be too large (Josey et al, 1996). The model equatorial stresses appear to be too strong in the Pacific when compared with the ECMWF analysis and ship winds (not shown). This has important implications for the ocean upwelling on the equator and for the simulation of SSTs in the coupled model.

The annual mean wind stress curl from the model and HR is shown in figs.12d and 12e. The overall pattern of the curl is well reproduced by the model and the positioning of the zero curl is represented realistically. In the north Pacific the zero windstress curl in part defines the separation point of the Kuroshio western boundary current (Hulbert et al, 1996). In reality, and in the coupled model (see Section 5), the Kuroshio extension is coincident with the region of high horizontal SST gradient The overall curl magnitudes are generally smaller in the model, compared to HR, which is consistent with the differences already noted in the stress magnitudes. The annual mean wind stress curl from the coupled model, meaned over the years 81-120, is shown in fig.12f. The wind stress curl zero line has moved south in the western north Pacific when compared to the simulation described above with prescribed SSTs. This movement is consistent with the coupled model SST errors in the Kuroshio extension region of the north Pacific (figs.6a and 6b). Additional sensitivity experiments in which the ocean model was forced with HR climatological stresses suggest that this southward movement of the Kuroshio separation is a consequence of the model wind stress distribution. With the HR stresses the separation point was located further to the north and therefore closer to its observed position. In both the atmosphere only and coupled model there are considerably higher meridional gradients in the Southern Ocean, compared to HR, and these are associated with the strong model stresses in this region.

6.2 The net surface heating

The net heat flux at the surface has four components; the net short wave and long wave fluxes, the latent heat flux associated with surface evaporation, and the sensible heat flux. The short wave and latent heat fluxes are the dominant contributions both in terms of magnitude and geographical variation. The net annual mean surface heating from the AMIP simulation and the corrected DS climatology are shown in figs.13a and 13b respectively. The corrections to the DS climatology are made to ensure a global balance of the surface heat budget (see Da Silva, 1994 for details). A contour interval of 50 Wm^{-2} has been used in order to highlight the main features. The difference plot in fig.13c has a smaller contour interval ($20Wm^{-2}$) to show greater spatial detail.

From figs.13a and 13b it can be seen that the major pattern features are well simulated by the model. In detail there are, however, some notable differences evident in fig.13c. For comparison, fig.13d shows the difference between the DS uncorrected total heat flux and the same quantity from the climatology of Josey et al (1996). The uncorrected climatologies are used so that the differences in fig.13d are only due to the detailed calculation methods and not the correction procedures. There is a difference between the climatologies of around 10-20 Wm^{-2} over much of the ocean which gives some measure of the level of uncertainty in the observational estimates.

The difference field in fig.13c shows that in the tropical east Pacific and Atlantic of the southern hemisphere the model has too much heat into the ocean surface. This is

particularly marked on the equator in the east Pacific, where the climatology shows the maximum heating some distance from the coast (fig.13b), whereas the model shows a large heating all the way to the coast (fig.13a). This feature is associated with the poor simulation of marine stratocumulus in these areas. A similar feature is also evident in the tropical Atlantic stratocumulus region. Fig.14a shows the difference in the net shortwave flux between the model and DS. Both the Atlantic and Pacific regions referred to above stand out as having an excessive short wave heat flux at the surface. Note that the Californian stratocumulus region also shows up clearly in the short wave difference map.

Some other notable differences in fig.13c are the tropical and sub-tropical regions in the north Pacific where there is more heat entering the ocean in the model than suggested by DS. Immediately under the peak of the trades this bias is reversed and the model exhibits a greater cooling than DS. In this region the overall increased heating over a broad area is a result of the larger surface short wave flux in the model (fig.14a), which is compensated for in the peak of the trades by enhanced surface evaporation (fig.14b). In the Indonesia/east Indian Ocean region the model gains too much heat mainly as a consequence of the enhanced short wave flux, by more than 50 Wm^{-2}, in some areas.

The difference between the mean net surface heating in the coupled model for the years 361 - 400 and the AMIP simulation of the same quantity (fig.13a) is shown in fig.15. The region of strong equatorial Pacific heating extends further west in the coupled model and is more intense due to the excessive upwelling of cold water on the equator, which leads to a reduced surface evaporation. The excessive upwelling is consistent with too strong low level equatorial winds. Note also the large flux differences associated with the changed position of sharp horizontal SST gradient in the model. These regions are associated with the northern oceans boundary currents and the ACC. In the North Pacific, where there is the largest SST error in the model, there is less heat loss in the coupled model than in the AMIP simulation due to a reduction in surface evaporation as the SST cools. Note also the greater cooling in the Pacific and Atlantic stratocumulus regions associated with the increased SST, and therefore surface latent heat loss, in the coupled model.

The large uncertainties in the climatological estimates need to be considered when assessing the comparisons made above. In particular, from a comparison of figs.14a and 14b, showing the shortwave and latent heat flux difference fields between the model and corrected DS, it is apparent that there is a net bias between the model and Da Silva. The model shortwave fluxes are everywhere larger than those from DS, whereas the latent heat fluxes are in many regions larger in the model, leading to some cancellation. The net long wave heat losses (not shown) are also generally larger in the model than in corrected DS, globally by about 7 Wm^{-2}. Despite these limitations, the coupled model SST drifts shown in the previous section do, to some degree, corroborate the analysis of model flux systematic errors as presented here.

Both the climatological and modelled surface heat fluxes can easily be integrated to give the implied ocean heat transports. These transports are plotted in fig.16 (coupled model transports are also shown on the figure and will be discussed in the next section). In both cases for simplicity of comparison the heat transport at 65°N was

assumed to be 0.1 PW (Da Silva, 1994). The un-corrected DS climatology has a global imbalance of 30 Wm^{-2} and the heat transports from the un-corrected fields are therefore meaningless. The DS heat transport curve plotted in fig.16 is from the corrected climatology which has a constraint of a zero global mean net heating imposed. The implied heat transport curve is therefore closed. The AMIP simulation has a net top of atmosphere (TOA) imbalance of 3.5 Wm^{-2}, much of which will be reflected in the imbalance of the global mean surface heating (Pope et al, 1998) and the implied ocean heat transport is therefore not closed.

For comparison with DS the model curve included in fig.16 uses the AMIP model transports that have been adjusted to ensure a zero global mean net surface heating. There is considerable similarity between the corrected transports from the model and climatology. The largest differences occur in the southern hemisphere, in particular, in the sub-tropics. The role of the excessive heat input in the stratocumulus (Sc) regions in the AMIP simulation in determining the discrepancies in the southern hemisphere sub-tropical transport can be assessed by artificially correcting the heat input in these Sc regions back to DS. This calculation suggests that between the equator and 15°S an additional flux of approximately 0.4 PW of heat is entering the ocean in the AMIP simulation compared to DS. At 15°S this would account for 80% of the discrepancy in the implied ocean heat transport shown in fig.16.

7. Validation of the Ocean Heat Transports in the Coupled Model

In this section we consider the ability of the model to reproduce the geographical distribution of global ocean heat transports when compared with direct ocean observations.

7.1 Global distribution of poleward heat transports

In the AMIP simulation present day SSTs and atmospheric greenhouse gas concentrations were used and a correction was applied to ensure a global mean balance when plotting the implied ocean heat transports. In the coupled model pre-industrial gas concentrations are employed which reduce the TOA flux imbalance by approximately 1.5-2.0 Wm^{-2}. Therefore the global mean imbalance at the start of the coupled simulation is approximately half the imbalance in the AMIP experiment.

Shown on fig.16 are a number of estimates of model poleward ocean heat transport from near the beginning of the simulation, and after 100 and 400 years. The calculation of implied equilibrium heat transports from the coupled model surface fluxes for years 1-10, 81–120 and 361-400 are also shown. Note also that in fig.16 the assumption of 0.1 PW heat transport at 65°N has not been made in plotting the curve from the coupled model, in fact, the model suggests a transport of approximately 0.25 PW at this latitude. For comparison the ocean heat transports as calculated within the ocean component of the coupled model are also included in fig.16 for the same time periods. As noted earlier in Section 2 the long term mean estimates of heat transports from the surface fluxes and from the ocean model must agree as the model reaches equilibrium. A critical issue is whether this state can be achieved whilst maintaining a realistic climate simulation in other respects.

One of the striking features of the heat transport curves in fig.16 is the short timescale for the coupled model transport to adjust away from the value implied in the AMIP

simulation. The rapid adjustment in the first decade is consistent with the equally rapid adjustment of the net TOA flux in the coupled model. This fast adjustment can also be seen in the SST, where the major characteristics of the SST pattern are established in the first 10 years.

Although the actual and implied heat transports differ by up to 0.2 PW in the sub-tropics, comparison of fig.16 with the equivalent plot for the earlier flux adjusted versions (HadCM2 and UKTR) in fig.1, shows that there is a much greater consistency in the new model between the atmospheric model surface fluxes and the ocean heat transports.

The modelled mean global heat transports for the years 361 - 400 are shown again in fig.17 and are broken down into component parts due to the zonal mean meridional overturning circulation, the gyre circulation (defined as the deviation from the zonal mean), the along isopycnal diffusive component and the Gent and McWilliams (1990) eddy transports.

The meridional overturning flux contains the contribution from the near surface Ekman transport, and this dominates in the tropics. In the model the contribution from the along isopycnal diffusive term and from the bolus velocity advection is small at most latitudes, and only makes a significant contribution to the zonal mean in the region of the Deacon Cell in the Southern Ocean. The smallness of the bolus advection term should not be interpreted as meaning the Gent and McWilliams parametrization does not influence the heat transports. What it shows, at least in this model, is that the most important aspect of the Gent and McWilliams parametrization is its ability to better maintain watermass properties (which comes about because of the absence of any background horizontal diffusion in the scheme), rather than it producing a significant heat flux directly due to eddies. The along isopycnal diffusive flux also makes a small contribution to the depth averaged meridional transport.

7.2 Comparison with Ocean Observations

To validate the modelled ocean heat transports the model results are compared with those obtained from direct ocean observations. Fig.18 shows the most recent direct estimates of meridional ocean heat transports from observations across the marked latitudes with the authors indicated by their initials. The stars indicate that the volume flux across the section is non-zero and the numbers indicate transports of temperature normalised to PW. The estimates are calculated from the instantaneous profiles of velocity and temperature measured on a single hydrographic section. For comparison, fig.19a and 19b show the advective heat transport across the marked latitudes for the mean of years 81-120 and 361-400 from the coupled model. In addition to the observed sections shown in fig.18, some extra model sections have been included in figs.19a and 19b. The model estimates are calculated from the mean velocity and temperature profiles for this period.

Both the observational estimates and the model calculation assume that the eddy heat flux is small compared with the large scale advective heat transport and the assumption is also made that the velocity and temperature profiles measured on a single hydrographic section are representative of the long-term mean velocity and temperature profiles.

A comparison of the heat transport for the two time periods (years 81-120 and 361-400) shows there to be a reduction in the Atlantic heat transport by O(0.1 PW) in the later period, while transports in the other basins are generally unchanged. Comparing figs.18 and 19a suggests that in the North Atlantic and North Pacific the ocean heat transports produced by the coupled model are in reasonable agreement with the observational estimates. In the South Atlantic the model shows less divergence in the heat transport than the observational estimates suggest, and the magnitude of the northward heat transport near 30°S is larger than all the published estimates with the exception of that by Fu (1981) of 0.8 PW (not shown). For a fuller discussion of the model heat transports in the South Atlantic see Banks (1998).

In the Indian and Pacific oceans we calculate temperature, rather than heat, transports (heat transports are invariant under a change of temperature scale, while temperature transports are not) since the mass transport across the basin is non-zero due to the presence of the Indonesian Throughflow (ITF). In the Indian Ocean the temperature transport is southwards as seen in the observations but is larger in magnitude, while in the South Pacific the temperature transport is in the opposite direction to most of the observations. These differences are associated with the magnitude of the ITF in the model, 24 Sv, larger than the observational range of 0-20 Sv (Wijffels et al, 1996), and dominates the temperature transports in the basins. The combined Indo-Pacific heat transports are in reasonable agreement with the observations.

7.3 Comparison with the Atlantic and Pacific 24°N Sections

To further validate the model a more detailed comparison of the components contributing to the total heat transports has been carried out for the sections at 24°N in the Atlantic and the Pacific. These 24°N sections are considered to provide robust observational estimates of the ocean heat transport because they are located in the centre of the sub-tropical gyre and the eddy heat transport is considered small compared to the total heat transport. Table 1 gives the breakdown of the total heat transport into its western boundary component (WBC), Ekman (wind driven) and interior components. In the model the WBC is defined by maximising the volume transport from the western boundary.

Table 1: Values for the heat transport components (PW) for the 40 year mean of years 81-120 from HADCM3 and the range (based on the decadal means for years 81-120). The total heat transport is split into components in two different ways: a) Western Boundary Current (WBC)/Ekman/Interior and b) Overturning/Gyre.

Atlantic 24°N

	Obs	**40yr mean**	**Range**
WBC	1.73	2.00	1.95 - 2.02
Ekman	0.42	0.28	0.27 - 0.29
Interior	-0.93	-1.14	-1.15 - -1.10
Total	1.22	1.14	1.12 - 1.16
Overturning	1.28	1.07	1.04 - 1.09
Gyre	-0.06	0.07	0.08 – 0.07

Pacific 24°N

	Obs	40yr mean	Range
WBC	1.73	2.32	2.23 - 2.37
Ekman	0.93	0.67	0.66 - 0.68
Interior	-1.91	-2.49	-2.41 - -2.55
Total	0.76	0.50	0.49 - 0.51
Overturning	0.38	0.14	0.13 - 0.16
Gyre	0.38	0.36	0.36 – 0.35

Comparing the components from HadCM3 at 24°N with the observational estimates of Hall and Bryden (1982) for the Atlantic, and Bryden et al. (1991) for the Pacific, we can see similar differences for both sections; an overestimate of the heat transported northward by the WBC and of the heat transported southward by the interior and an underestimate of the heat transported northward by the Ekman layer. The underestimate of the Ekman layer heat transport is related to the reduced Ekman transport across the section; 3.8 Sv (Atlantic) and 7.5 Sv (Pacific), compared with 5.0 Sv (Atlantic) and 12.0 Sv (Pacific) in the observational estimates. The observational estimates are based on the climatological windstresses from Hellerman and Rosenstein (1983) which may bias the Ekman transport to larger values (for example, across 24°N in the Pacific, calculating the Ekman transport from the Josey et al (1996) climatology rather than HR leads to a reduction of 3 Sv). The remaining 1.5 Sv discrepancy between model and observations is relatively small.

The overturning component of the heat transport in HadCM3 is 1.07 PW for the Atlantic, accounting for 93% of the total heat transport (compared with the observational estimate of 1.28 PW accounting for 105% of the total). In the Pacific, the overturning component is 0.14 PW accounting for 28% of the total (compared with the observational estimate of 0.38 PW which accounts for 50% of the total). In both cases, not only is the magnitude of the overturning component smaller than the observed estimate but it suggests a greater role for the gyre component in the model than is indicated by the observations. In particular, the gyre component is southward in the observations (since the WBC is generally colder than the interior) while in the model the gyre component is northward.

Boning et al (1996) compared the strength of the North Atlantic Deep Water (NADW) cell at 25°N with the poleward heat transport at the same latitude, from a variety of models with different resolutions and forcings. Although there is a considerable range amongst the models in the value of the heat transport at 25°N, there is a simple linear relationship between the strength of the NADW cell and the poleward heat transport that fits all the model results. The overturning meridional/depth streamfunction for the North Atlantic in the coupled model for the periods years 81-120 and 361-400, is shown in figs.20a and 20b. The strength of the NADW cell is stable, whereas a

deeper cell clearly 'spins up' over the 400 years of the integration. The strength of the NADW cell at 24°N is between 16 - 18 Sv, with a corresponding heat transport of 1.1 PW. These values also fit the simple relationship between the overturning and heat transport in Boning et al (1996). Hall and Bryden (1982) estimate the magnitude of the NADW cell to be 19 Sv (integrating their table 5).

The volume transports at 24°N in the Atlantic can also be compared with observations for different temperature classes. Table 2 shows the transports in temperature classes for the model during the years 81-120 and 361-400 compared with the observational estimate of Hall and Bryden (1982).

Table 2: Northward Volume Transport in Temperature Classes (Sv)

	Hall and Bryden Observed	Years 81-120	Years 361-400
$\theta > 17°C$	8.9	13.8	11.4
$12 < \theta < 17°C$	2.5	0.6	0.9
$7 < \theta < 12°C$	6.6	1.3	3.1
$4 < \theta < 7°C$	-2.3	-6.8	-16.4
$\theta < 4°C$	-15.6	-8.8	2.0

Compared with Hall and Bryden, HadCM3 transports more water northwards in the warmest temperature class and less in the two classes below this. By the later period, about 2 Sv of warmest water has moved to the cooler temperature classes.

For the earlier period, there is some indication of southward flow of NADW moving to the temperature class $4 < \theta < 7°C$. This trend appears to continue, so that during the later period all NADW transport is in the warmer class. This is consistent with the reduction in northward heat transport between the two periods and with the shallower depth of the NADW cell in the later period.
Overall, the adjustment of the transport in temperature classes is consistent with a reduction in the effective temperature difference of the overturning.

In summary, the overturning cell in the Atlantic is slightly too weak in HadCM3 when compared to Hall and Bryden (1982). This is consistent with the difference in total heat transport of O(0.1 PW) between model and observed as predicted by the simple linear relationship in Boning et al (1996). The larger magnitude in the observations may be partly attributable to the Ekman transport calculated from HR which is larger than the model Ekman transport. Macdonald (1995) found that reducing the Ekman transport from 5.4 Sv (from HR stresses) to 4.2 Sv (ECMWF stresses) reduced the total heat transport by 0.13 PW. Finally, the percentage of the heat transport explained by the overturning and gyre components is probably related to the structure of the western boundary current in the model. With a horizontal resolution of 1.25° the boundary currents cannot be simulated realistically.

8. Summary

The HadCM3 Hadley Centre coupled model has a much improved SST and sea ice climatology compared to earlier models in which flux adjustments were necessary to prevent large climate drifts. One of the key features in this advance has been the improved simulation of the surface heat fluxes and the poleward heat transports, which in the HadCM3 model are in broad agreement with the observed estimates. This was not the case in earlier versions of the model. In HadCM3 the heat transports needed by the atmospheric component to maintain its present day climate agree reasonably well with the heat transports simulated by the ocean model. As suggested by Weaver and Hughes (1996) this leads to a stable model. Boville and Gent (1998) and Bryan (1998) also conclude that this consistency of fluxes is, in part, responsible for the stability of their 300 year simulation with the un-flux adjusted CSM1 model. They also attribute the stability to the initialisation procedure used. In HadCM3 we have no pre-coupled initialisation and this is clearly not a pre-requisite for a stable coupled model simulation.

We can conclude the following:

a) The atmospheric model, run in atmosphere-only mode, is capable of a realistic simulation of the surface heat flux field. This in itself is a significant achievement in atmospheric model performance. One major limitation here is the quality of the flux climatologies used to validate the model.

b) When coupled, the ocean model approximately maintains the poleward heat transports as implied by the atmosphere only case. That is, the system is self consistent and there is no need for the SST to undergo large drifts in order to rebalance the heat budget. Flux adjustments are therefore not required and the coupled model can be initialised directly from an observed ocean state without the need for separate equilibriation of the ocean model.

c) The ocean component of the coupled model simulates poleward heat transports in broad agreement with estimates from oceanographic sections.

The SST pattern in the model stabilises after only a few decades. The sea ice simulation is encouraging and the improvement in ocean heat transports in the model has an important consequence in improving the position of the ice edge. The thermohaline circulation in the model is stable although it does show significant variability (Wood et al, 1998).

The main emphasis of this study has been the validation of the surface heat exchange and ocean heat transport processes in the coupled model. It is important in coupled models that this kind of analysis is carried out to ensure that the mechanisms in the model, at least those in determining the mean balanced state, are realistic. This is necessary if we are to have confidence in numerical experiments to understand climate and predict climate change using such models.

Appendix: Data transfer between grids

Particular problems in the techniques for exchanging information between the ocean and the atmosphere arise from the models being on different horizontal grids. The information passed from the ocean to the atmosphere describes the state of the surface (temperature and sea ice parameters). Because the sea ice fields can have sharp discontinuities, bilinear interpolation from the higher- resolution ocean grid is not considered satisfactory. Instead, we use an area-weighted average of the six ocean gridboxes, which cover the area of each atmosphere gridbox, making full use of all the information available.

The information passed from the atmosphere to the ocean describes the surface fluxes of momentum, heat and fresh water. It is essential that the coupling should be conservative i.e. the area-average of each quantity on the two grids must be equal. We could set the six ocean points in an atmosphere box all equal to the single atmosphere value for the box, but we prefer to have ocean fields which vary continuously in space. To achieve both these aims, we first use bilinear interpolation from the atmosphere grid to obtain a field which varies on the higher-resolution ocean grid. Then we calculate the area-average of the six ocean boxes in each atmosphere box, and compare it with the atmosphere value. Since interpolation is not conservative, the values will not generally be equal. We adjust the six ocean values by dividing by the ratio of the average to the atmosphere value, or subtracting the difference, to regain equality in each atmosphere box. Division is used for positive-definite quantities, such as downward penetrative shortwave radiation (subtraction might give unphysical negative values), and addition for others, such as net surface water flux (where there might be six nearly balancing values of opposite signs, and division by their small sum could produce unreasonably large values). This adjustment procedure depends on the coincidence of the ocean and atmosphere land-sea masks, so that both grids have the same ocean area in each atmosphere box.

REFERENCES

Banks H T (1998) Ocean heat transport in the South Atlantic in a coupled climate model. To be submitted to JGR.

Barthelet P, Terray L and Valcke S (1998) Transient CO2 experiment using the ARPEGE/OPAICE non flux corrected coupled model. Geophys. Res. Lett. 25: 2277-2280.

Bigg GR, Wadley MR, Stevens DP and Johnson JA (1996) Prediction of iceberg trajectories in the North Atlantic and Arctic Oceans. Geophys. Res. Lett. 23: 3587-3590.

Boning CW, O.Bryan F, Holland WR and Doscher R (1996) Deep water formation and meridional overturning in a high resolution model of the north Atlantic. J. Phys. Oceanogr. 26:1142-1164.

Boville BA and Gent PR (1998) The NCAR Climate Systems Model, Version One. J. Climate, 11:1115-1130.

Bryan FO (1998) Climate drift in a multi-century integration of the NCAR Climate System Model. J. Climate, 11: 1455-1471.

Bryden HL, Roemmich DH and Church JA (1991) Ocean heat transport across 24°N in the Pacific. Deep Sea Res. 38: 297-324.

Cattle H and Crossley J (1995) Modelling Arctic Climate Change. Phil. Trans. R. Soc. Lond. A352: 201-213.

Cox P, Betts R, Bunton C, Essery R, Rowntree PR and Smith J (1998) The impact of new land surface physics on the GCM simulation of climate and climate sensitivity. Climate Dynamics to appear.

Cox MD (1984) A primitive equation, 3 dimensional model of the ocean. GDFL Ocean Group Technical Report No 1, Princeton NJ, USA, 143pp.

Cusack S, Slingo A, Edwards JM and Wild M (1998) The radiative impact of a simple aerosol climatology on the Hadley Centre Atmospheric GCM. QJR Meteor. Soc. To appear.

Da Silva AM, Young C and Levitus S (1994) Atlas of Surface Marine Data, NOAA Atlas NESDIS 6. [Available from US Dept. of Commerce]

Edwards JM and Slingo A (1996) Studies with a flexible new radiation code. I: Choosing a configuration for a large scale model. QJR Meteor. Soc. 122: 689-719.

Fevrier S, Frankignoul C, Sirven J, Davey MK, Delecluse P, Ineson S, Macias J, Sennechaek N, Stephensom DB (1998) A multivariate intercomparison between oceanic GCMs using observed current and thermocline depth anomalies in the tropical Pacific during 1985-92. Submitted to J. Geophys. Res.

Fu L.-L. (1981) The general circulation and meridional heat transport of the subtropical South Atlantic determined by inverse methods. J. Phys. Oceanogr.11: 1171-1193.

Gates WL (1992) AMIP: The Atmospheric Model Intercomparison Project. Bull Amer. Met. Soc. 124: 1613-1646.

Gent P and McWilliams JC (1990) Isopycnal mixing in ocean circulation models. J. Phys. Oceanogr. 20:150-155.

Gibson JK, Kallberg P, Uppala S, Hernandez A, Nomura A, Serrano E (1997) ERA Description. ECMWF Re-Analysis Project Series 1.

Gill AE and Niiler PP (1973) The theory of the seasonal variability in the ocean. Deep Sea Res. 20:141-178.

Gordon C and Bottomley M (1985) The parametrization of the upper ocean mixed layer in coupled ocean/atmosphere models. Published in the proceedings of the 16th Leige Colloquim on Ocean Hydrodynamics, Ed. JCJ Nihoul, Elsevier.

Gregory D, Kershaw R, Inness PM (1997) Parametrization of momentum transport by convection II: Tests in single column and general circulation models. QJR Meteor. Soc. 123: 1153-1183.

Gregory D and Morris D (1996) The sensitivity of climate simulations to the specification of mixed phase clouds. Clim. Dyn.12: 641-651.

Gregory D, Shutts GJ and Mitchell JR (1998) A new gravity wave drag scheme incorporating anisotropic orography and low level wave breaking: Impact upon the climate of the UK Meteorological Office Unified Model. QJR Meteor. Soc. 124: 463-493.

Gregory JM and Mitchell JFB (1997) The climate response to CO2 of the Hadley Centre coupled AOGCM with and without flux adjustment. Geophys. Res. Lett. 15: 1943-1946.

Griffies SM, Gnanadesikan A, Pacanowski RC, Larichev VD, Dukowicz JK and Smith RD (1998) Isoneutral diffusion in a z-coordinate ocean model. J. Phys. Oceanogr. 28: 805-830.

Hall MM and Bryden HL (1982) Direct estimates and mechanisms of ocean heat transport. Deep Sea Res. 29: 339-359.

Haney RL (1971) Surface thermal boundary conditions for ocean circulation models. J. Phys. Oceanogr. 1: 241-248.

Harvey JG (1976) Atmosphere and ocean: our fluid environment (Artemis)

Hellerman, S and Rosenstein M (1983) Normal monthly wind stress over the world ocean with error estimates. J. Phys. Oceanogr.13: 1093-1104.

Houghton JT, Meira Filho LG, Callander BA, Harris N, Kattenberg A and Maskell K (1996) Climate Change 1995. The Science of Climate Change. Cambridge University Press.

Hulbert HE, Walleraft AJ, Schnitz WJ Jr, Hogan PJ and Metzyer EJ (1996) Dynamics of the Kuroshio/Oyashio current system using eddy-resolving models of the North Pacific Ocean. J. Geophys. Res. 101: 941-976.

Johns TC, Carnell RE, Crossley JF, Gregory JM, Mitchell JFB, Senior CA, Tett SFB and Wood RA (1997) The second Hadley Centre coupled ocean-atmosphere GCM: Model description, spinup and validation. Clim. Dyn. 13: 103-134.

Josey SA, Kent EC, Oakley D and Taylor PK (1996) A new global air-sea heat and momentum climatology. International WOCE Newsletter, 24: 3-5.

Kraus EB and Turner JS (1967) A one dimensional model of the seasonal thermocline II. The general theory and its consequences. Tellus 19: 98-105.

Levitus S and Boyer TP (1994) World Ocean Atlas 1994, Volume 4: Temperature. NOAA/NESDIS E/OC21, US Department of Commerce, Washington, DC, 117pp.

Levitus S, Burgett R and Boyer TP (1995) World Ocean Atlas 1994, Volume 3: Salinity. NOAA/NESDIS E/OC21, US Department of Commerce, Washington, DC, 99pp.

Macdonald AM (1995) Oceanic fluxes of mass, heat and freshwater: a global estimate and perspective. PhD thesis. 326pp, Mass. Inst. Of Technol./Woods Hole Oceanogr. Inst. Joint Programme, Woods Hole, Mass.

Manabe S, Stouffer RJ, Spelman MJ and Bryan K (1991) Transient responses of a coupled ocean-atmosphere model to gradual changes of atmospheric CO2. Part I: Annual Mean Response. J. Climate, 4: 785-818.

Martin GM, Johnson DW and Spice A (1994) The measurement and parametrization of effective radius of droplets in warm stratocumulus clouds. J. Atmos. Sci. 51: 1823-1842.

Milton SF and Wilson CA (1996) The impact of parametrized sub-grid scale orographic forcing on systematic errors in a global NWP model. Mon. Weath. Rev. 124: 2023-2045.

Moss SJ and Johnson DW (1994) Aircraft measurements to validate and improve numerical model parametrizations of ice to water ratios in clouds. Atmospheric Research 34:1-25.

Murphy JM (1995) Transient response of the Hadley Centre coupled ocean-atmosphere model to increasing carbon dioxide. Part I: Control climate and flux adjustment. J. Climate, 8: 36-56.

NSIDC (1989) DMSP SSM/I brightness temperatures and sea ice concentration grids for the polar regions. NSIDC Distributed Active Archive Centre, University of Colorado, Boulder, USA.

Pacanowski RC and SG Philander (1981) Parametrization of vertical mixing in numerical models of tropical oceans. J. Phys. Oceanogr.11: 1443-1451.

Pfirman SJ, Bauch D and Gammelsrod T (1994) The northern Barents Sea: Water mass distribution and modification, in The Polar Oceans and their role is shaping the global environment: The Nansen Centennial Volume, Geophys. Monogr. Ser., vol. 85, edited by OM Johannessen, RD Muench and JE Overland, pp 77-94, AGU, Washington DC.

Pope VD, Gallani ML, Rowntree PR, Stratton RA (1998) The impact of new physical parametrizations in the Hadley Centre climate model – HadAM3. Submitted to Climate Dynamics.

Rayner NA, Horton EB, Parker DE, Folland CK and Hackett PB (1996) Version 2.2 of the Global sea Ice and Sea Surface Temperature (GISST) data set, 1903-1994. Climate Research Tech. Note (CRTN) 74, Hadley Centre, Meteorological Office, Bracknell, UK.

Roether W, Roussenov VM and Well R (1994) A tracer study of the thermohaline circulation of the eastern Mediterranean. In Ocean Processes in Climate Dynamics: Global and Mediterranean Example pp.371-394. Eds. P. Malanotte-Rizzoli and AR Robinson, Kluwer Academic Press, 1994.

Russell GL, Miller JR and Rind D (1995) A coupled atmosphere-ocean model for transient climate change studies. Atmosphere-Ocean. 33: 683-730.

Sausen R, Barthel K and Hasselmann K (1988) Coupled ocean-atmosphere models with flux adjustment. Climate Dynamics, 2: 145-163.

Smith RNB (1990) A scheme for predicting layer clouds and their water content in a general circulation model. QJR Meteor. Soc.116: 435-460.

Smith RNB (1993) Experience and developments with the layer cloud and boundary layer mixing schemes in the UK Meteorological Office Unified Model. In Proceedings of the ECMWF/GCSS workshop on parametrization of the cloud-topped boundary layer, 8-11 June, 1993. ECMWF, Reading, England.

Thompson SR, Stevens DP and Doos K (1997) The importance of interocean exchange south of Africa in a numerical model. J. Geophys. Res.102, C2: 3303-3315.

Visbeck M, Marshall J, Haine T and Spall M (1997) On the specification of eddy transfer coefficients in coarse resolution ocean circulation models. J. Phys. Oceanogr. 27: 381-402.

Warrick et al (1996). Changes in sea level, in: Climate Change 1995: The Science of Climate Change. Cambridge University Press.

Weaver JW and Hughes TMC (1996) On the incompatibility of ocean and atmosphere models and the need for flux adjustments. Climate Dynamics, 12: 141-170.

White G (1996) Editor. WCRP workshop on air-sea flux fields for forcing ocean models and validating GCMs. WMO/TD – No.762.

Wijffels SE, Bray N, Hautala S, Meyers G and Morawitz W (1996)
The WOCE Indonesian Throughflow repeat hydrography sections: I10
and IR6. International WOCE Newsletter, 24: 25-28.

Wood RA, Keen AB, and Mitchell JFB (1998) Spatial variations in the stability of the North Atlantic thermohaline circulation under greenhouse gas forcing. To be submitted to Nature.

Wright DK (1997) A new eddy mixing parametrization and ocean general circulation model. International WOCE Newsletter, 26:27-29.

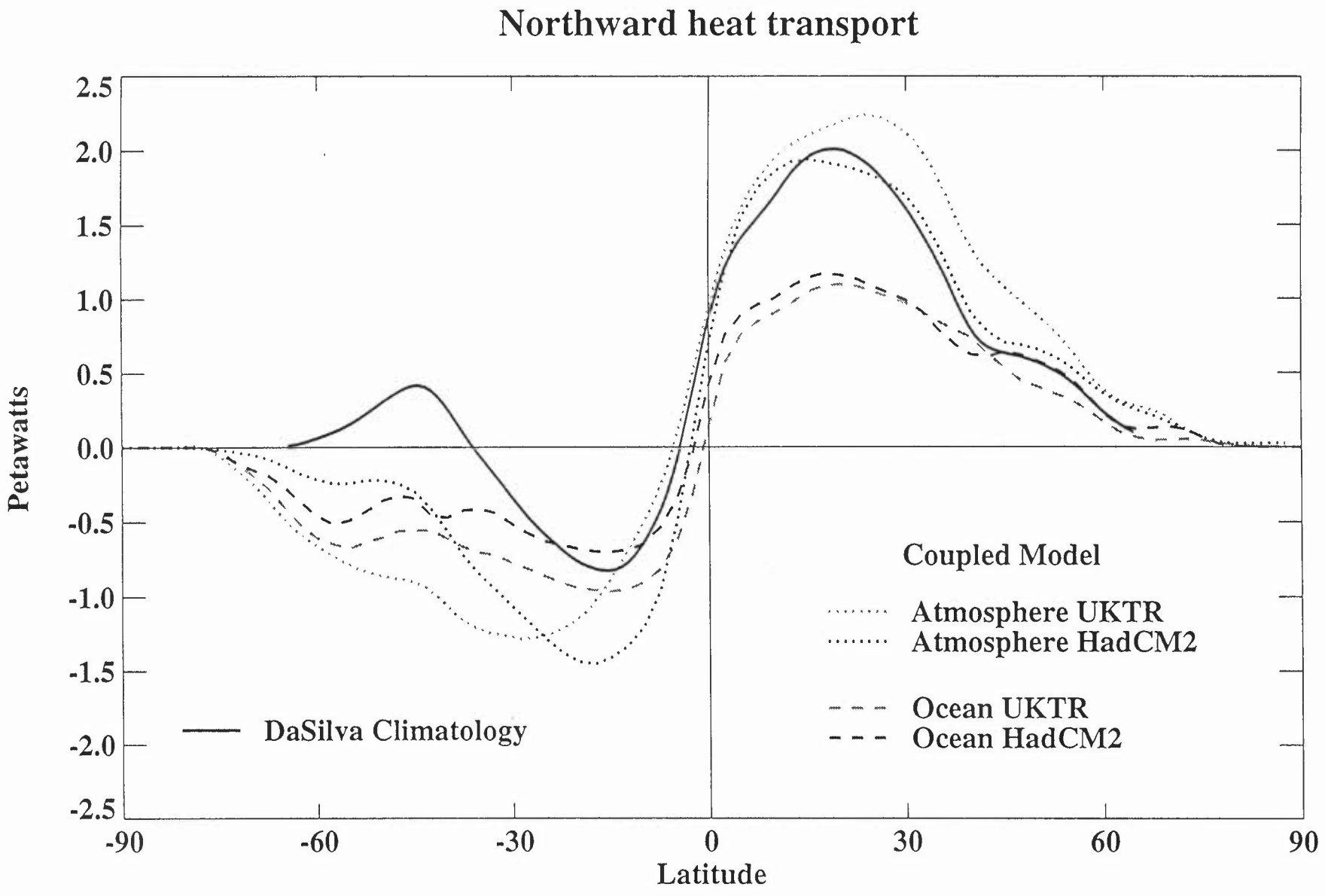

Fig.1 The northward heat transport as calculated from the atmosphere and ocean components of previous flux adjusted versions of the Hadley Centre model. Climatological estimates based upon the Da Silva et al (1994) compilation of surface fluxes are also included.

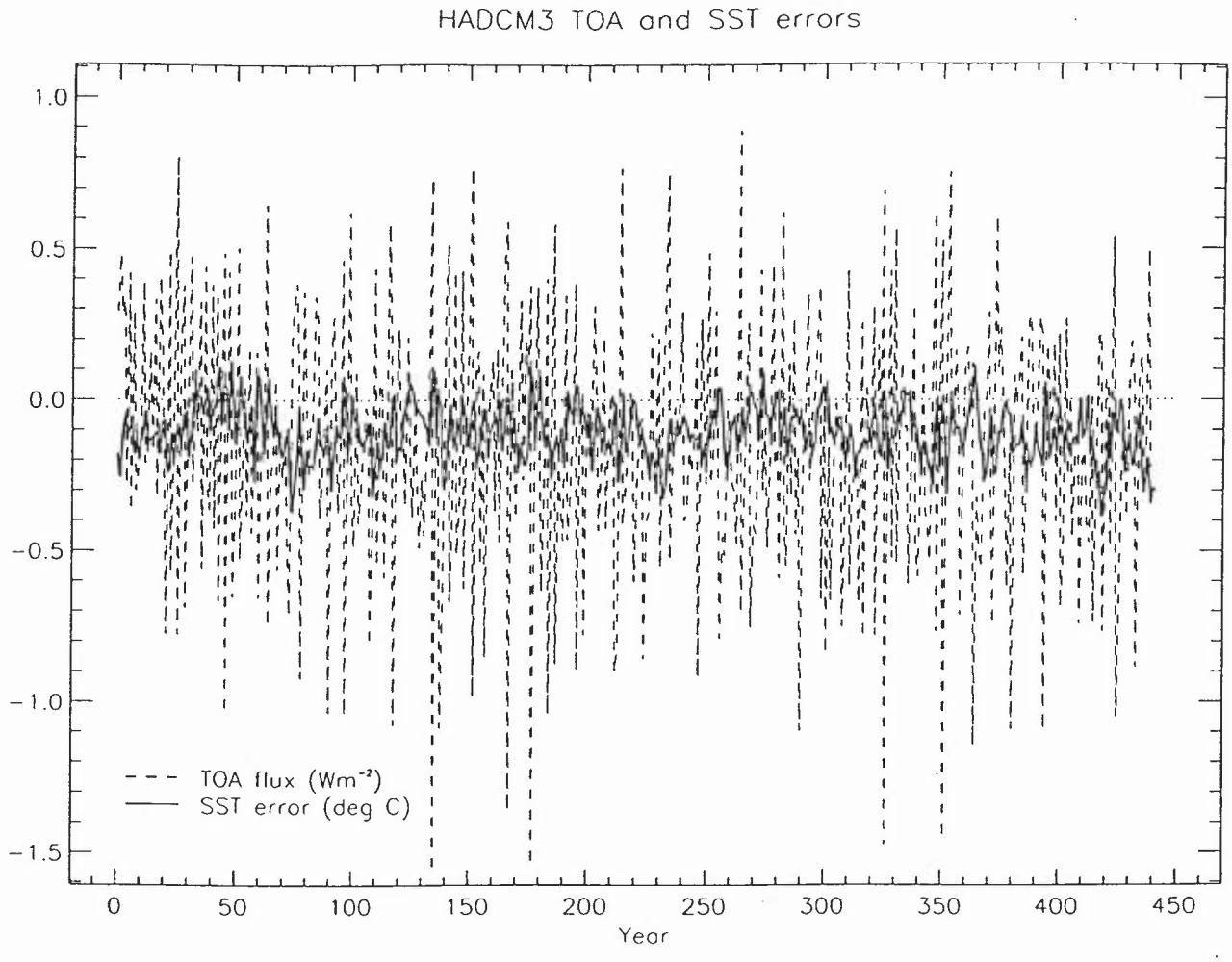

Fig.2 Timeseries of the global mean SST difference (°C) from climatology and the top of atmosphere flux imbalance (Wm^{-2}).

(a) Global Temperature Drift (°C)

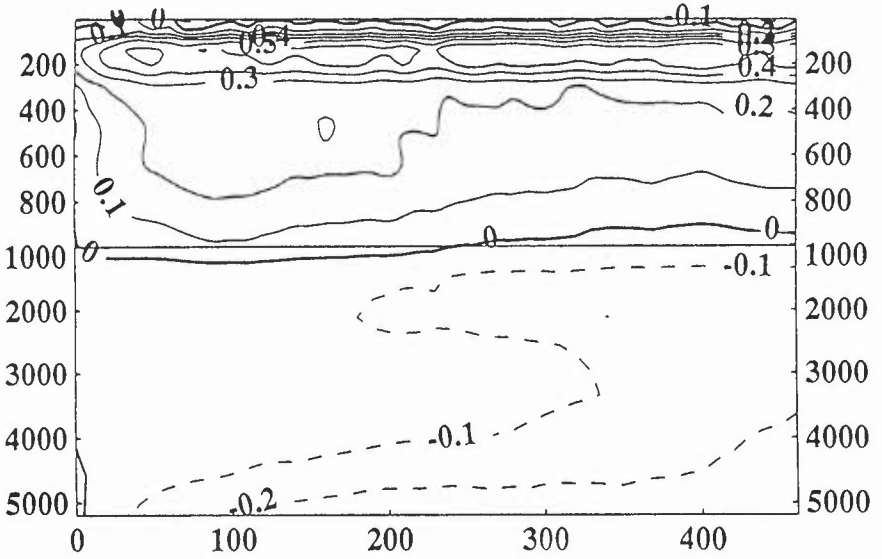

(b) Global Salinity Drift (ppt)

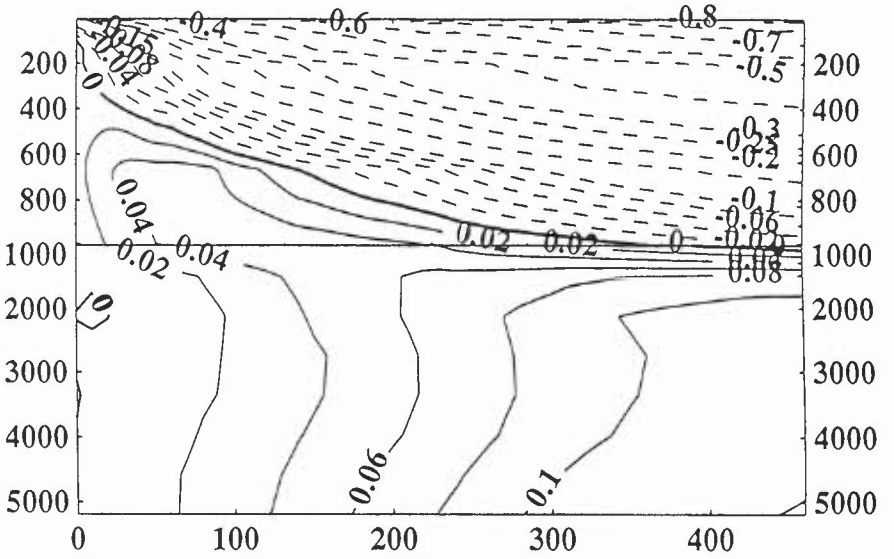

(c) Global volume weighted temperature (°C)

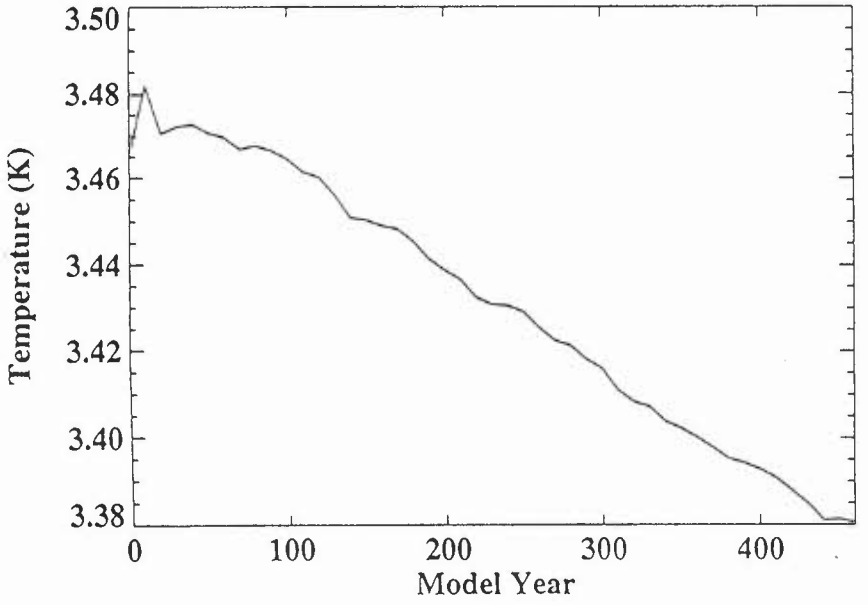

Fig.3 (a) Time/depth time series of global mean temperature drift (°C). Differences are calculated from the Levitus (1994) climatology and the upper 1000m has an expanded depth scale.
(b) As 3a but for salinity drift (ppt).
(c) Timeseries of global volume weighted temperature for the whole ocean (°C).

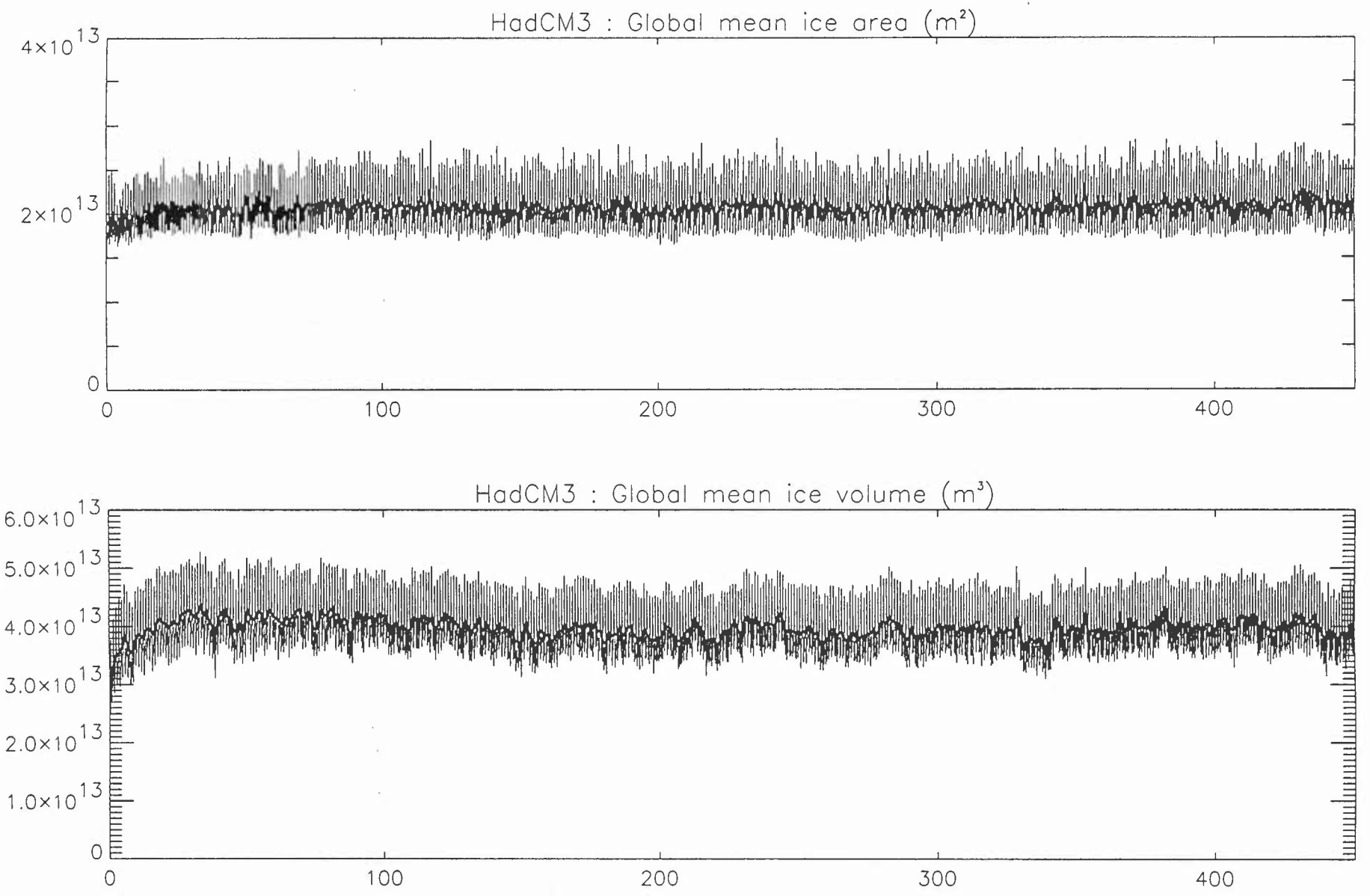

Fig.4 (a) Time series of global mean sea ice area (m^2).
(b) Time series of global mean sea ice volume (m^3).

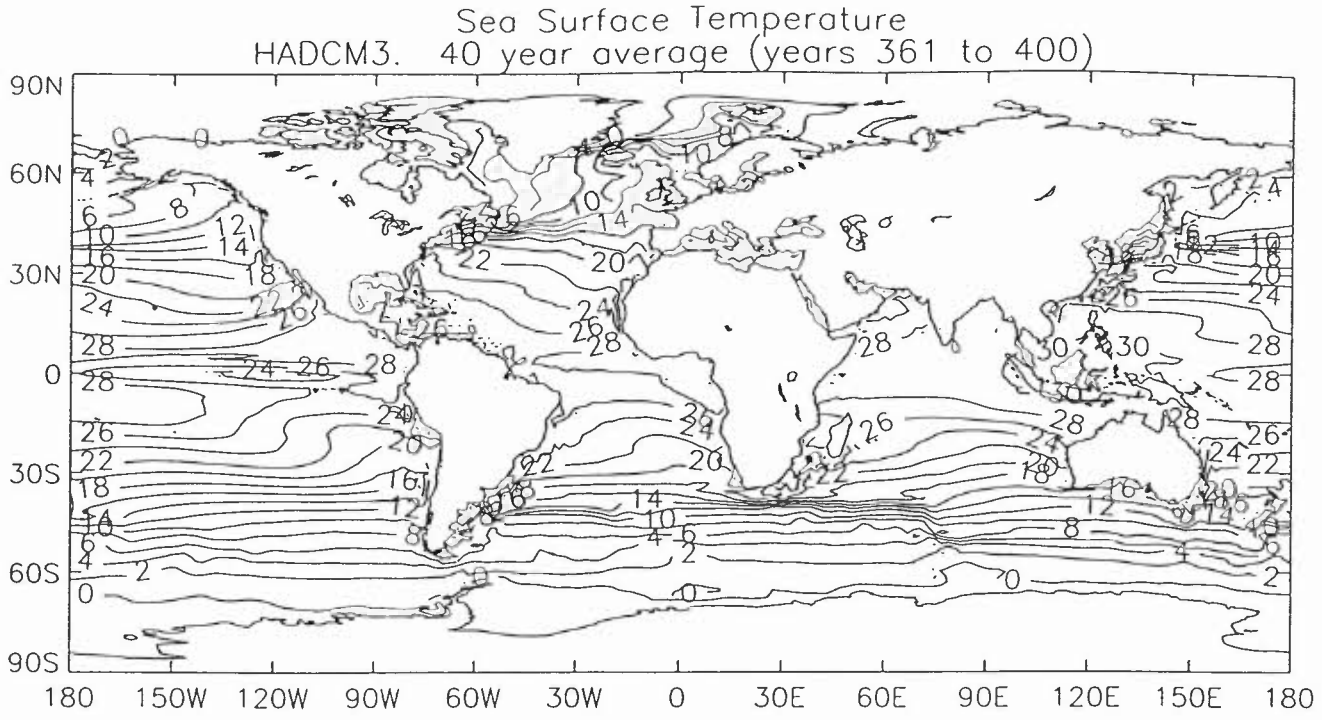

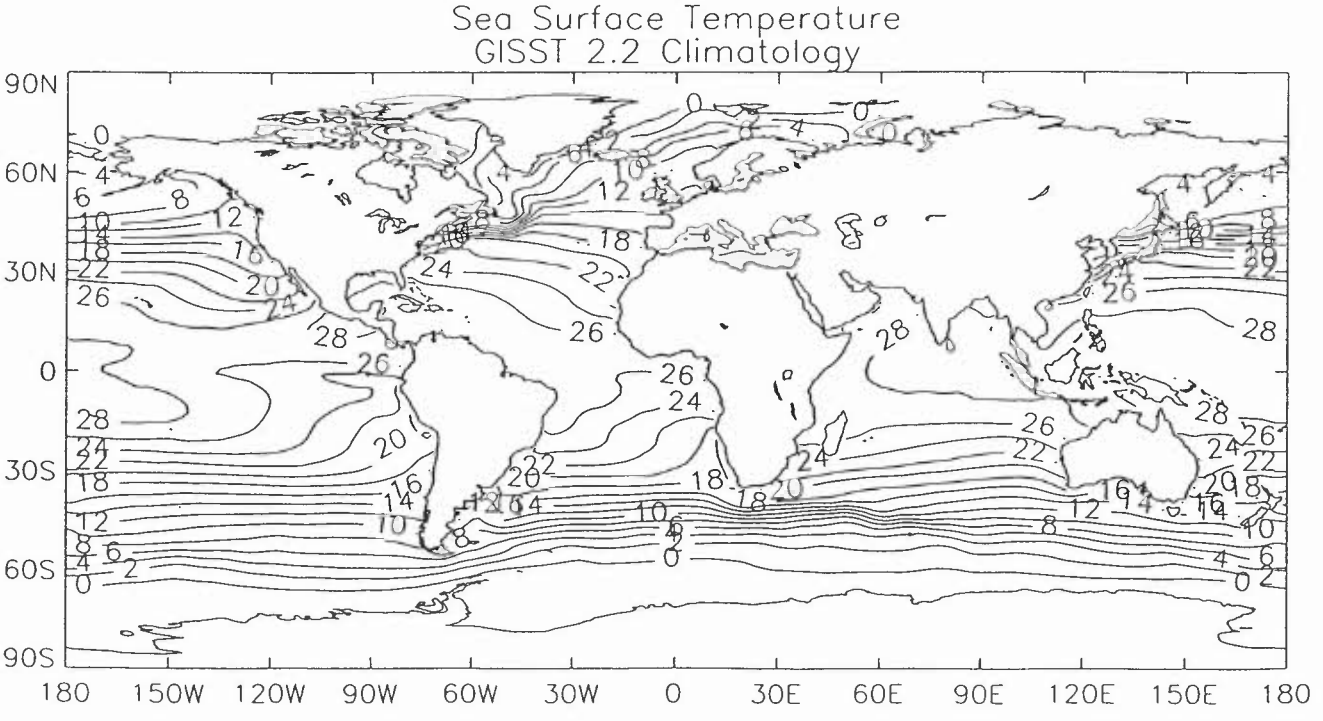

Fig.5 (a) The coupled model annual mean SSTs (°C) averaged over the years 361-400.

(b) The annual mean SST (°C) from the GISST2.2 climatology.

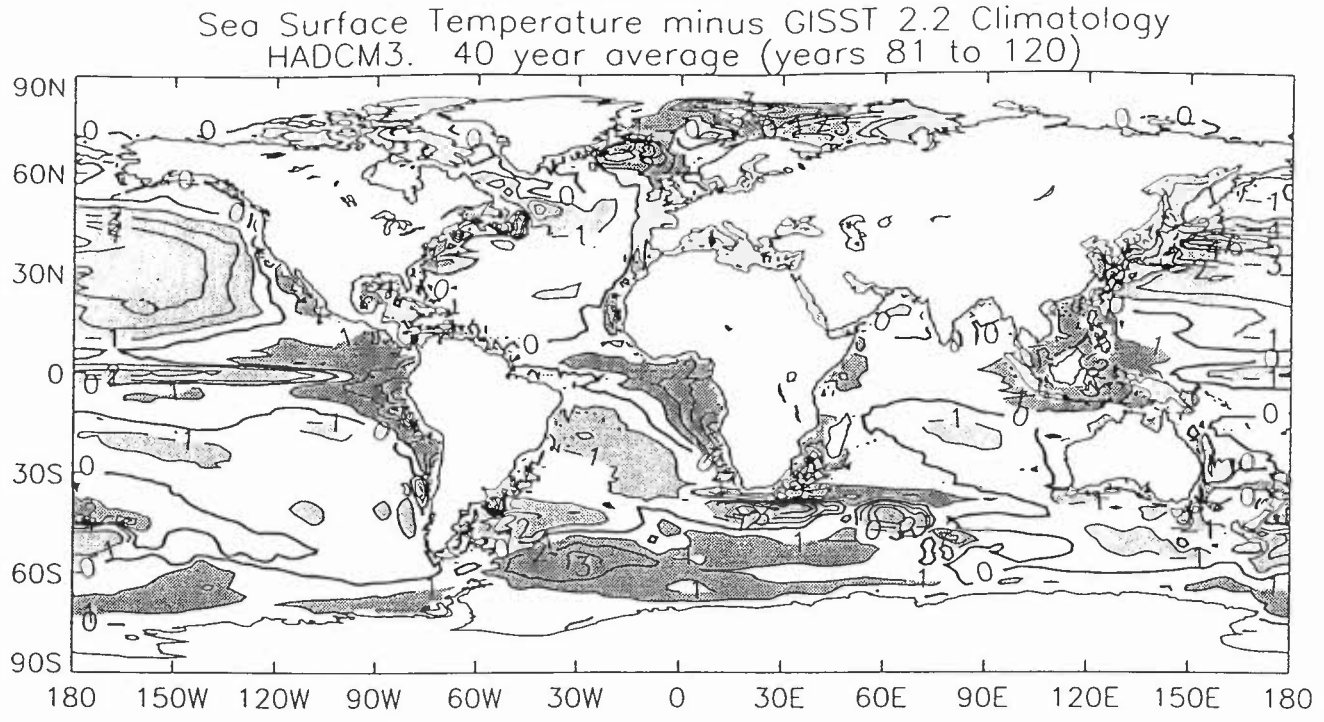

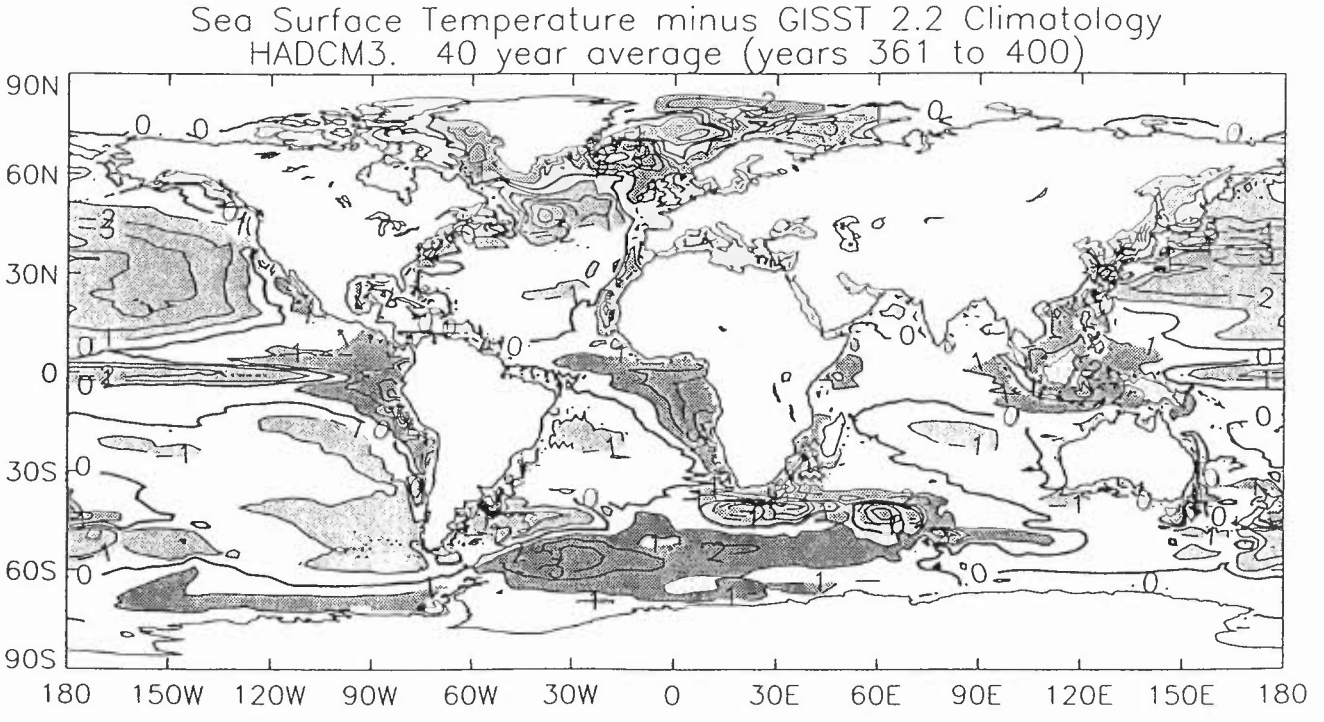

Fig.6 (a) The model minus climatology SST (°C) difference averaged over the years 81-120.
(b) As (a) but for the model years 361-400.

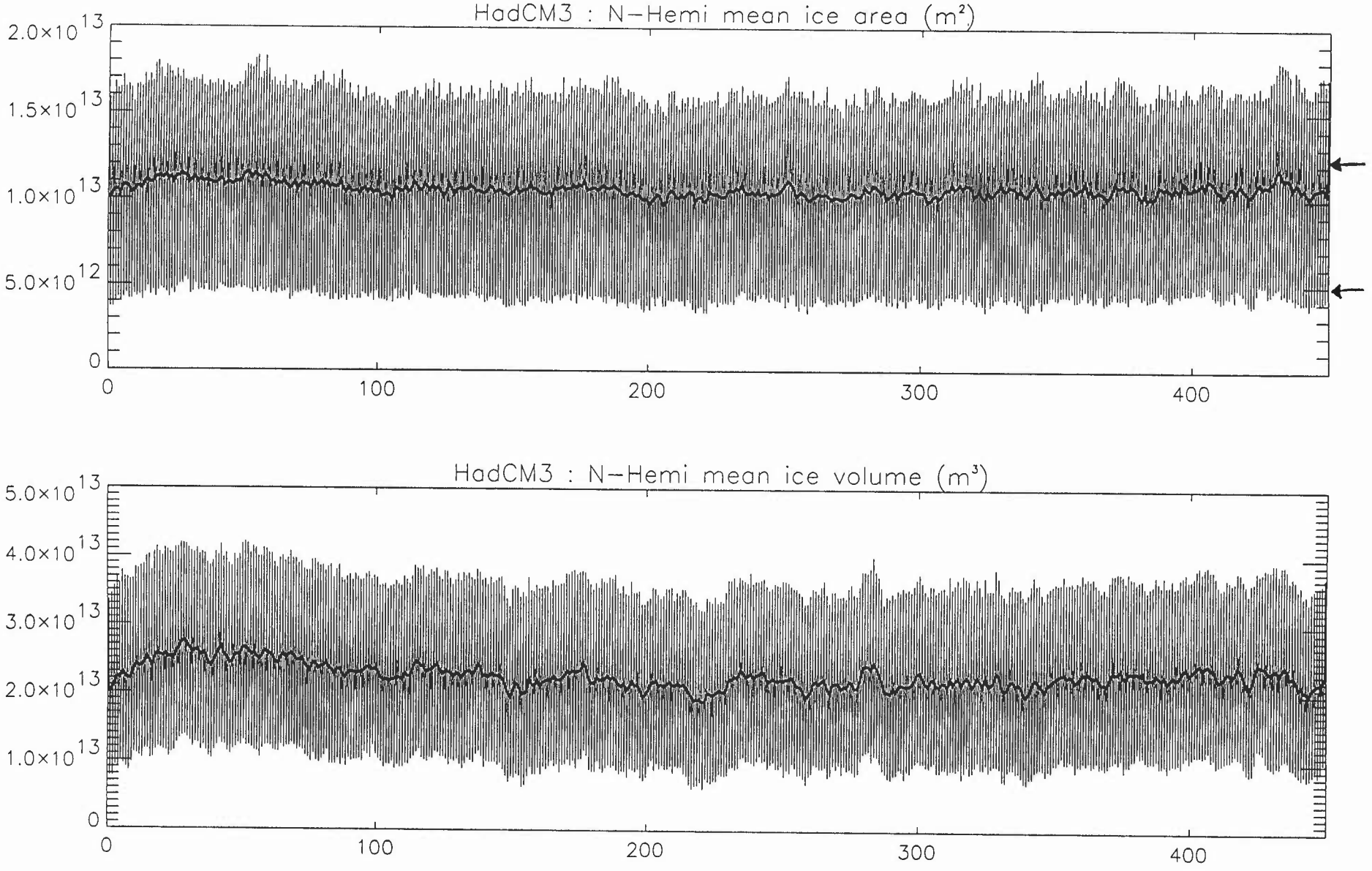

Fig.7 (a) Time series of northern hemisphere sea ice area (m^2). The thick line is the annual mean and the observed seasonal extents (arrows on rhs of figures) are from SSM/I data (NSIDC, 1989).
(b) Time series of northern hemisphere sea ice volume (m^3). The thick line is the annual mean.

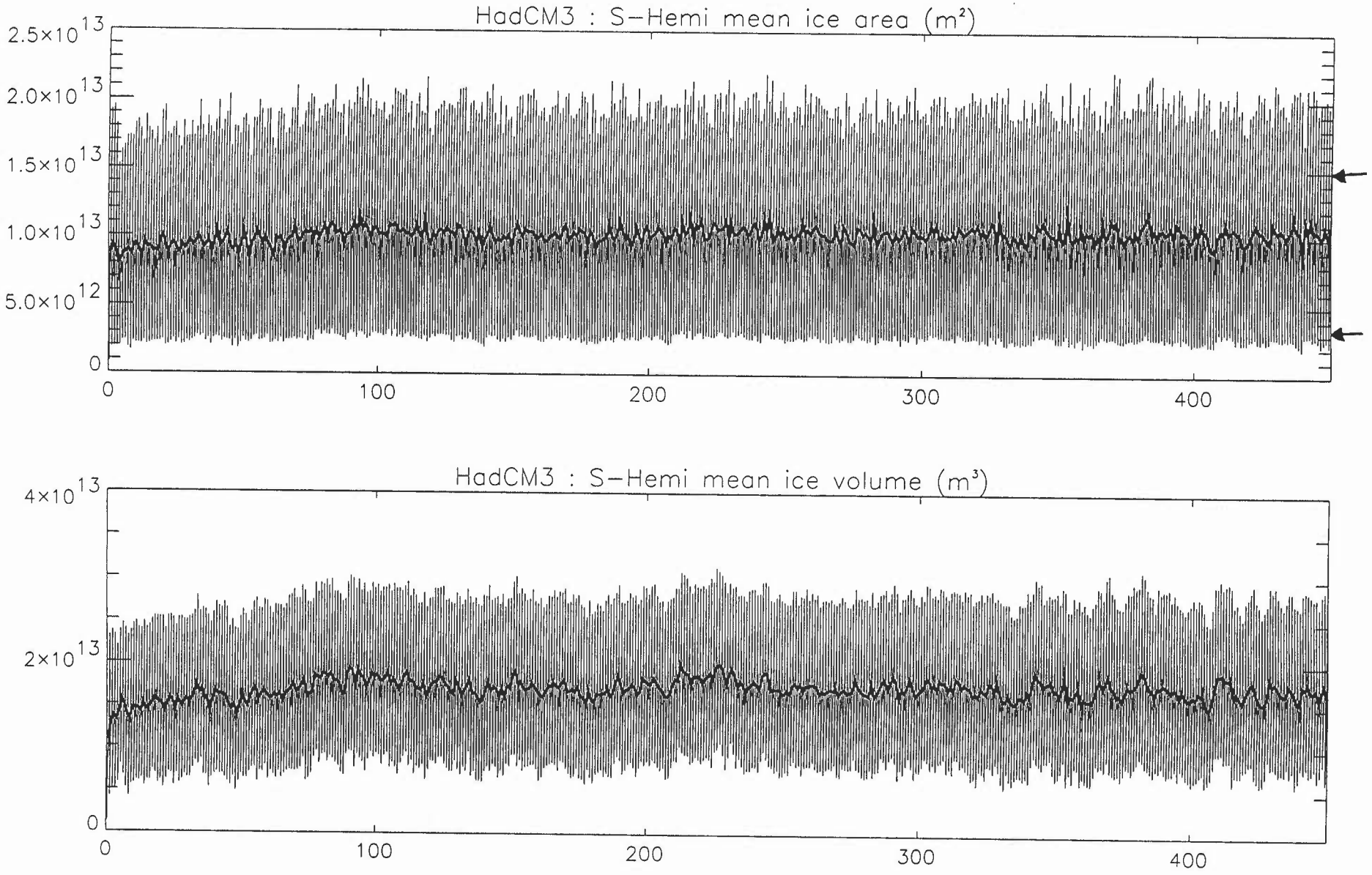

Fig.8 As fig.7 but for the southern hemisphere sea ice.

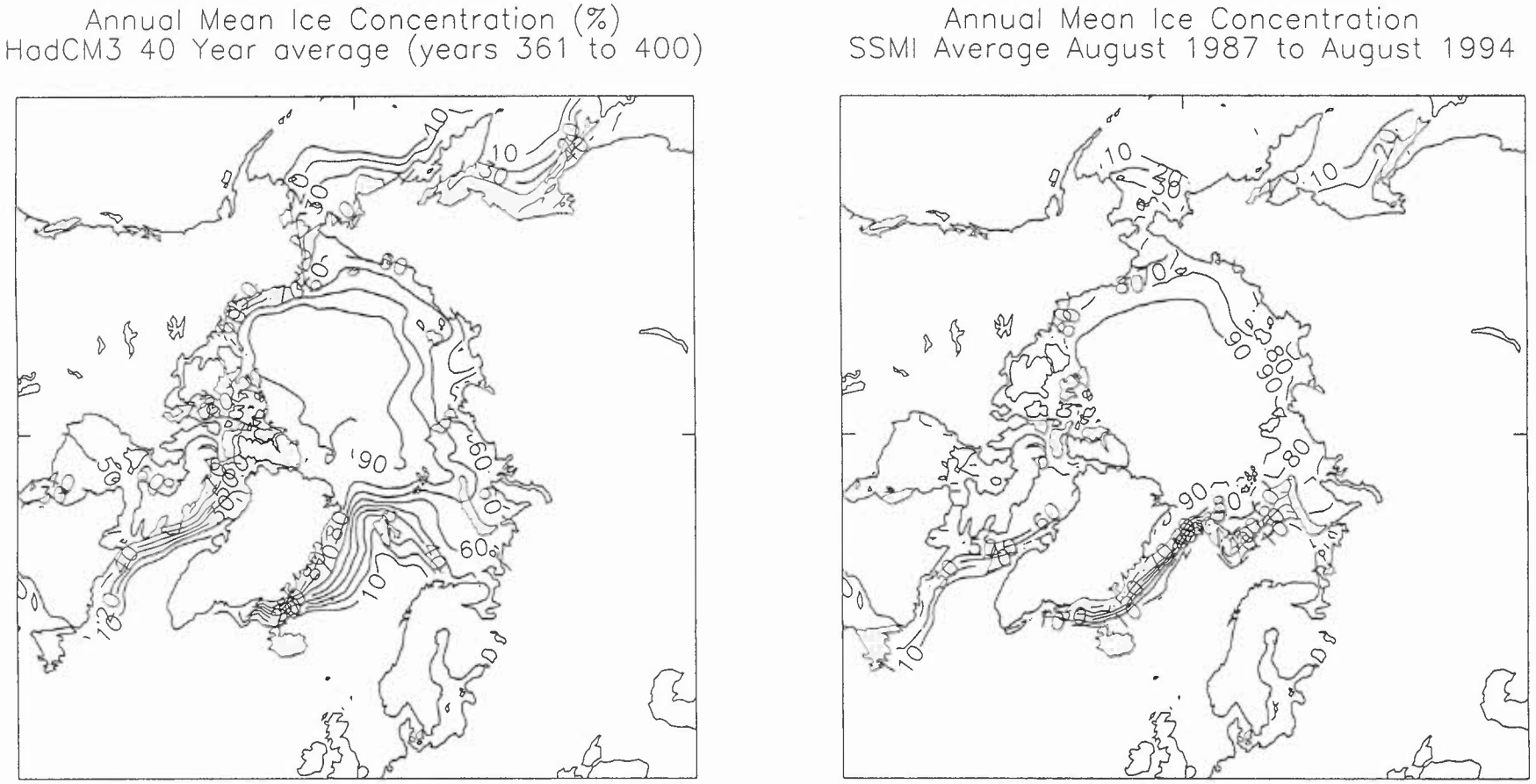

Fig.9 (a) Modelled annual mean northern hemisphere sea ice concentrations for the years 361-400. Concentration is plotted as a percentage and the contour interval is 10%.
(b) As (a) but from SSM/I data.

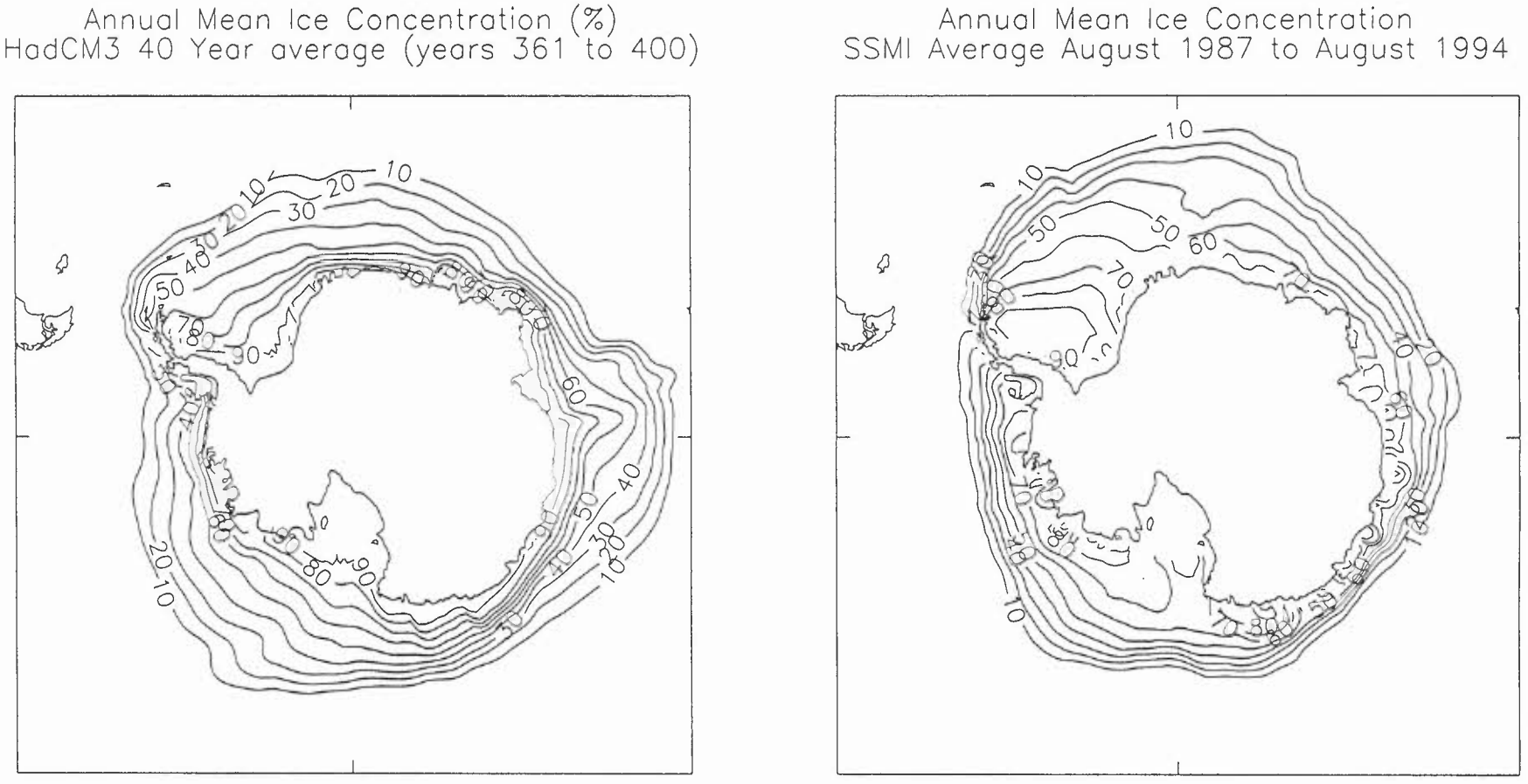

Fig.10 As fig.9 but for the southern hemisphere.

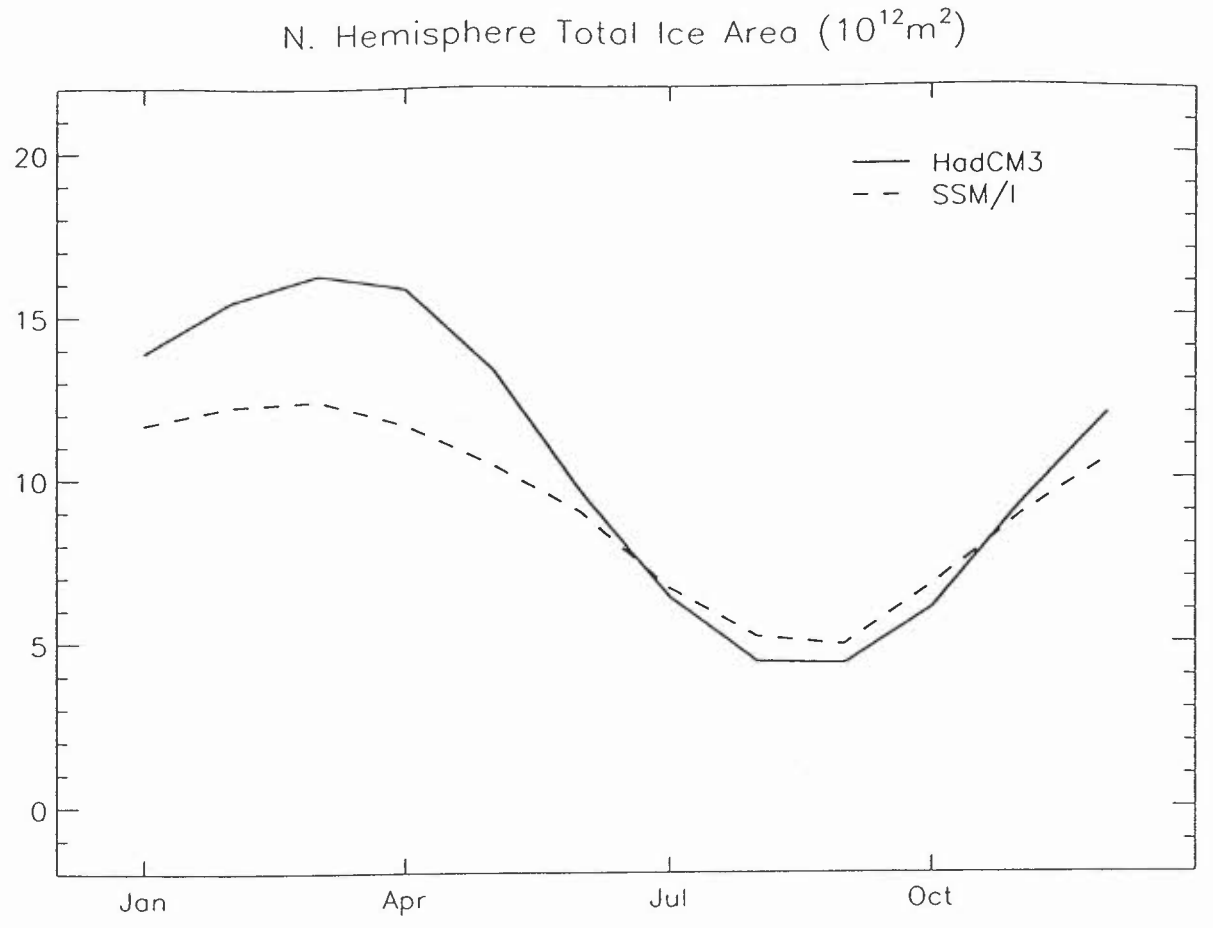

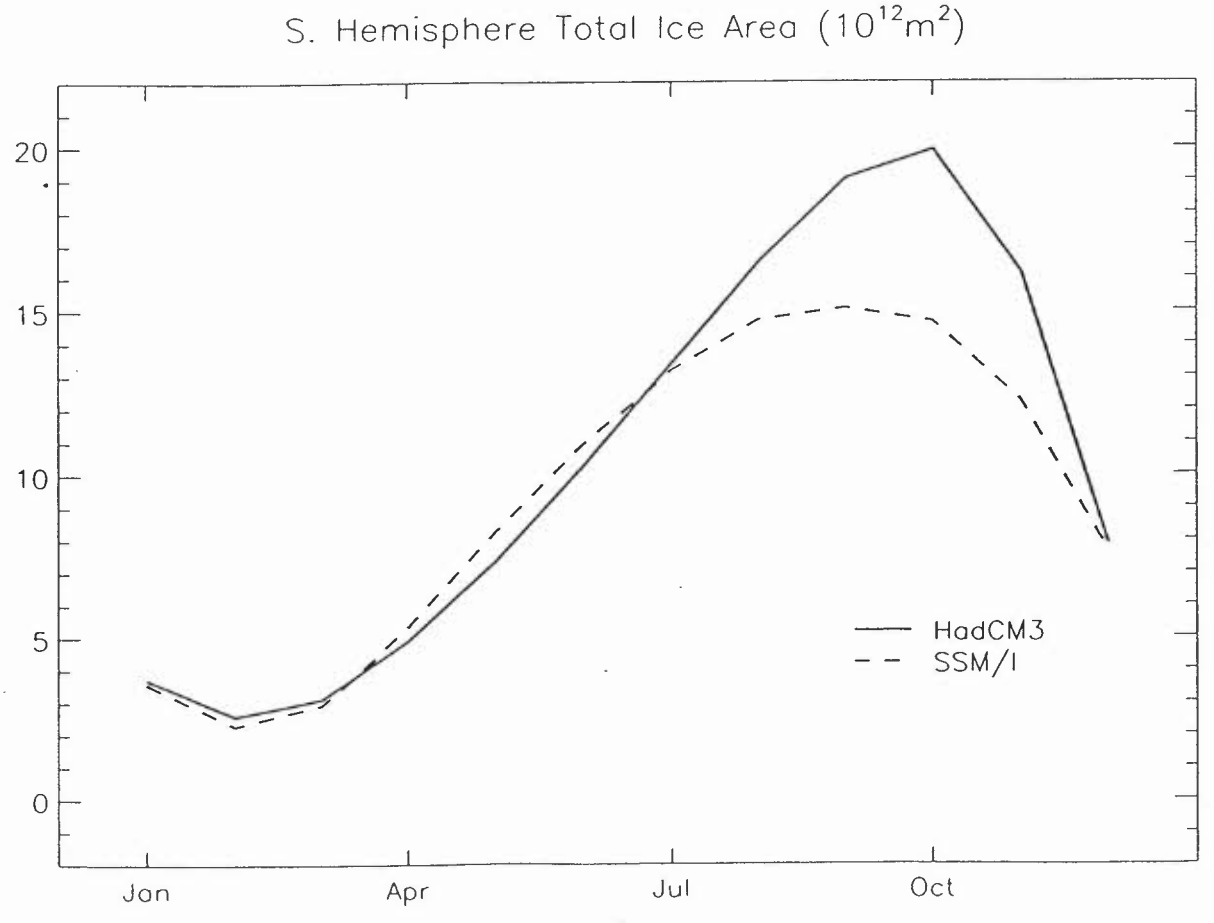

Fig.11 (a) The mean monthly seasonal cycle of northern hemisphere sea ice area for the model years 361-400 and from SSM/I data.
(b) As (a) but for the southern hemisphere.

(a)

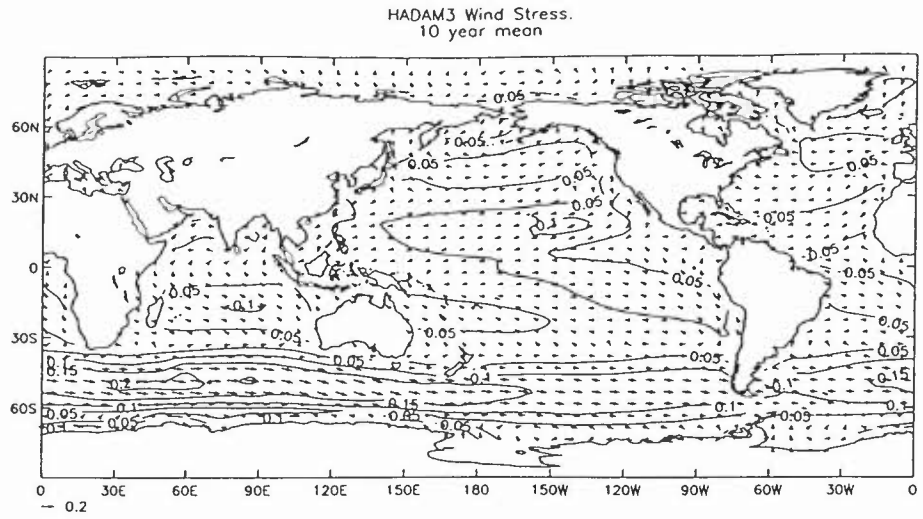

(b)

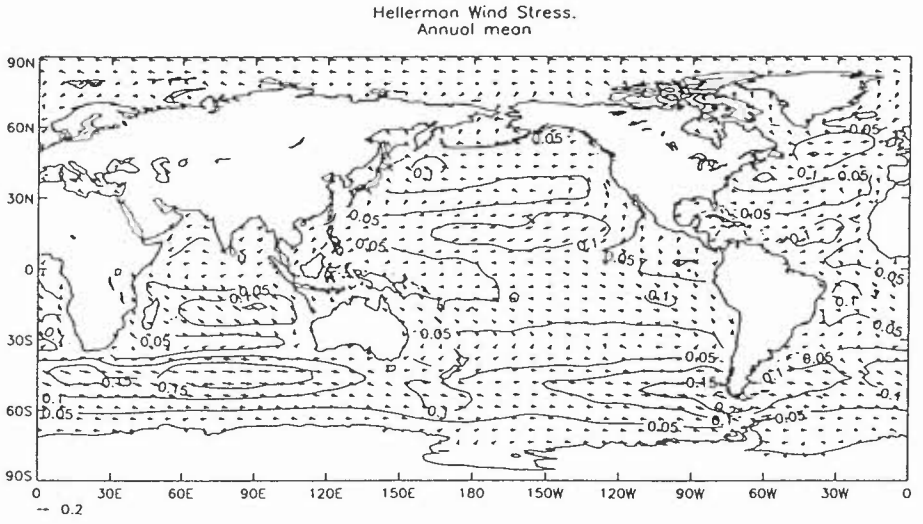

(c)

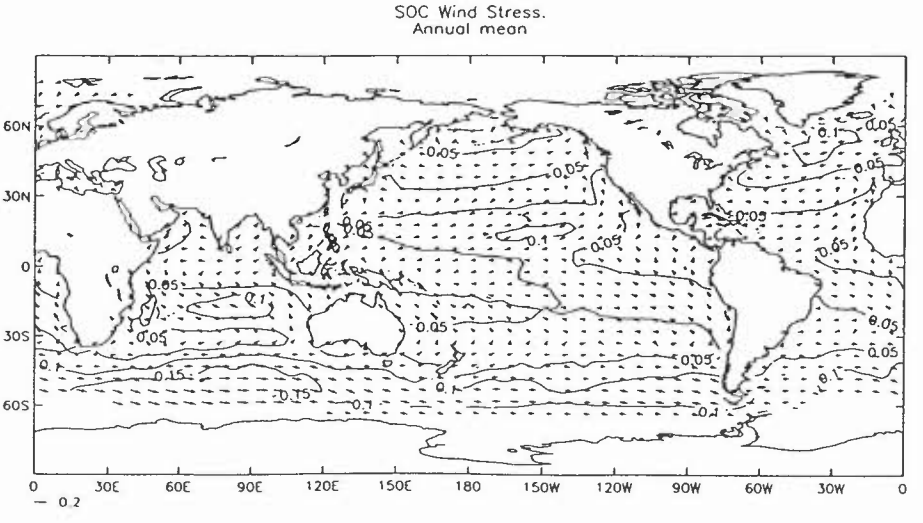

Fig.12 (a) Ten year annual mean surface stress (Nm^{-2}) from the AMIP simulation with the HadAM3 model.
(b) Annual mean surface stress from the HR climatology.
(c) Annual mean surface stress from the Josey et al (1996) climatology.

(d)

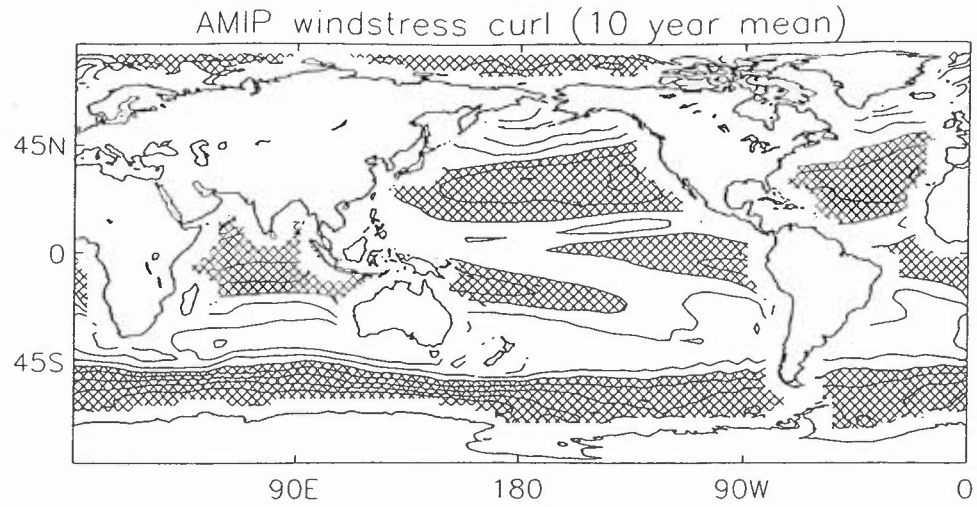

(e)

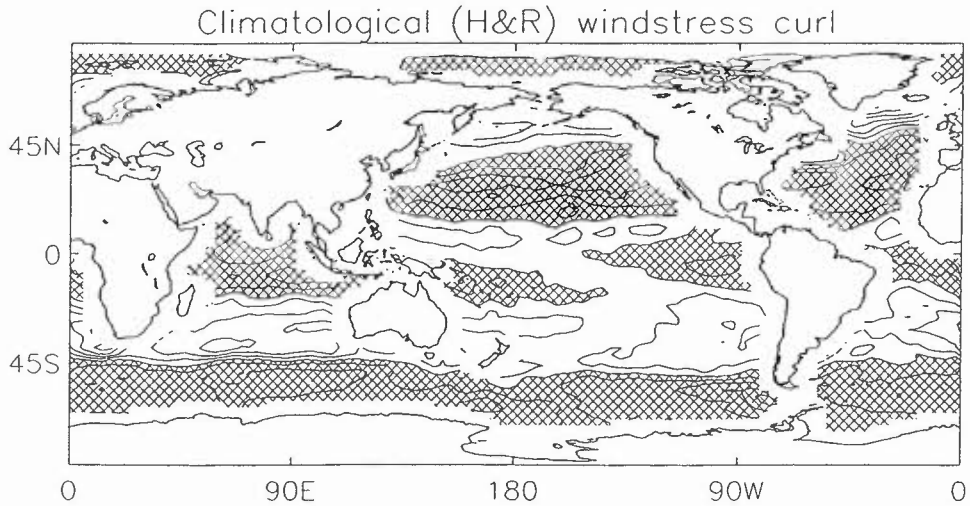

(f)

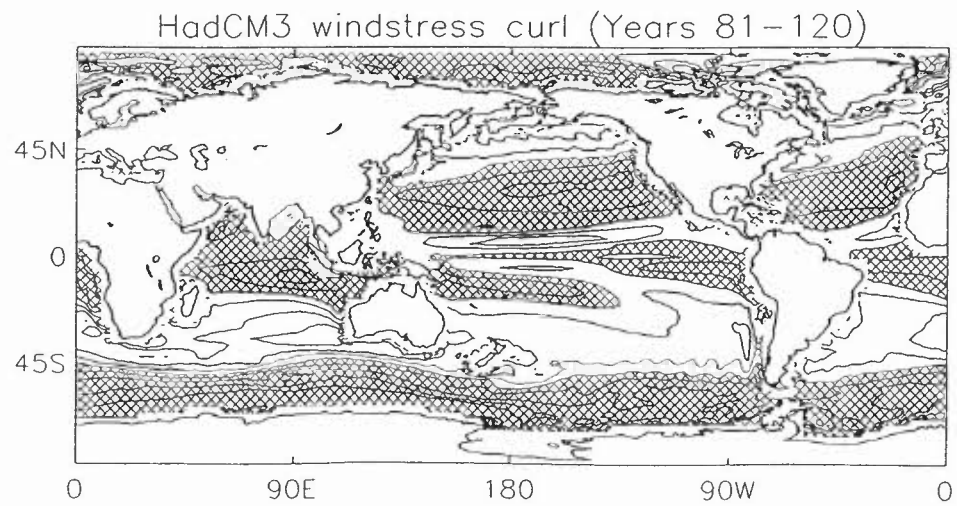

Fig.12 (d) Ten year mean windstress curl from the AMIP simulation with the HadAM3 model. (The contour interval is 0.5×10^{-7} Nm^{-3} and negative regions are shaded.)

(e) Wind stress curl from the HR climatology.

(f) Wind stress curl from years 81-120 of the HadCM3 coupled simulation

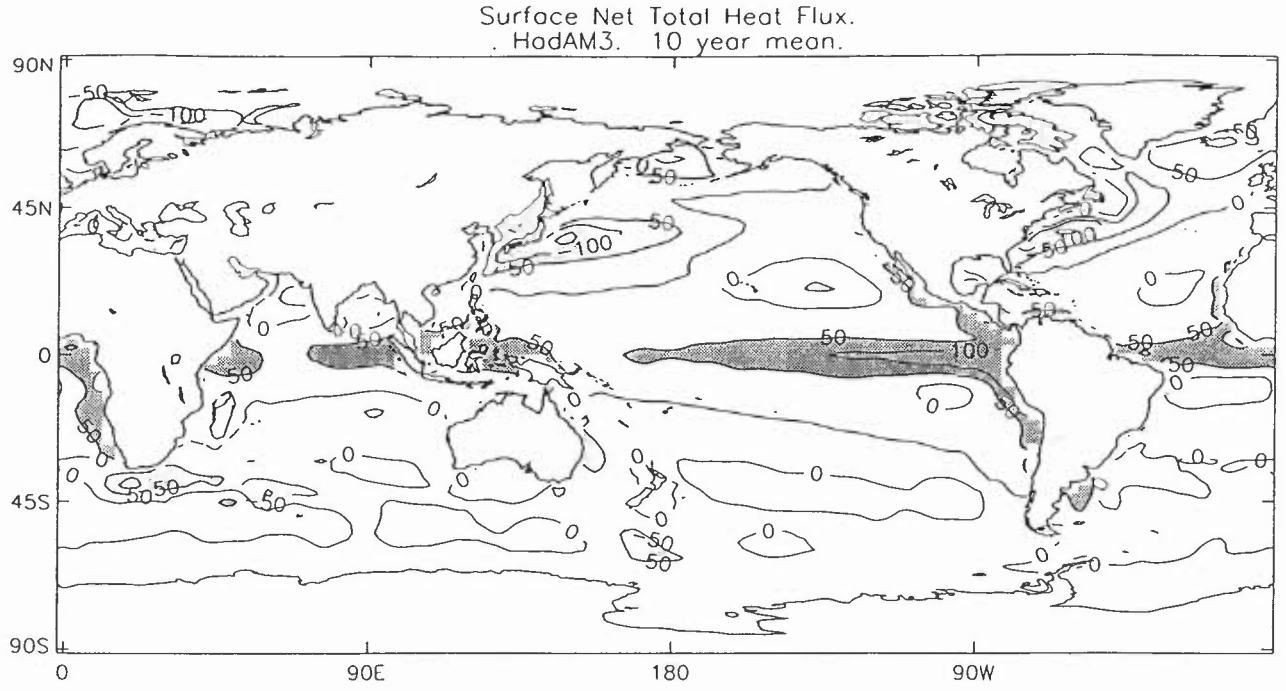

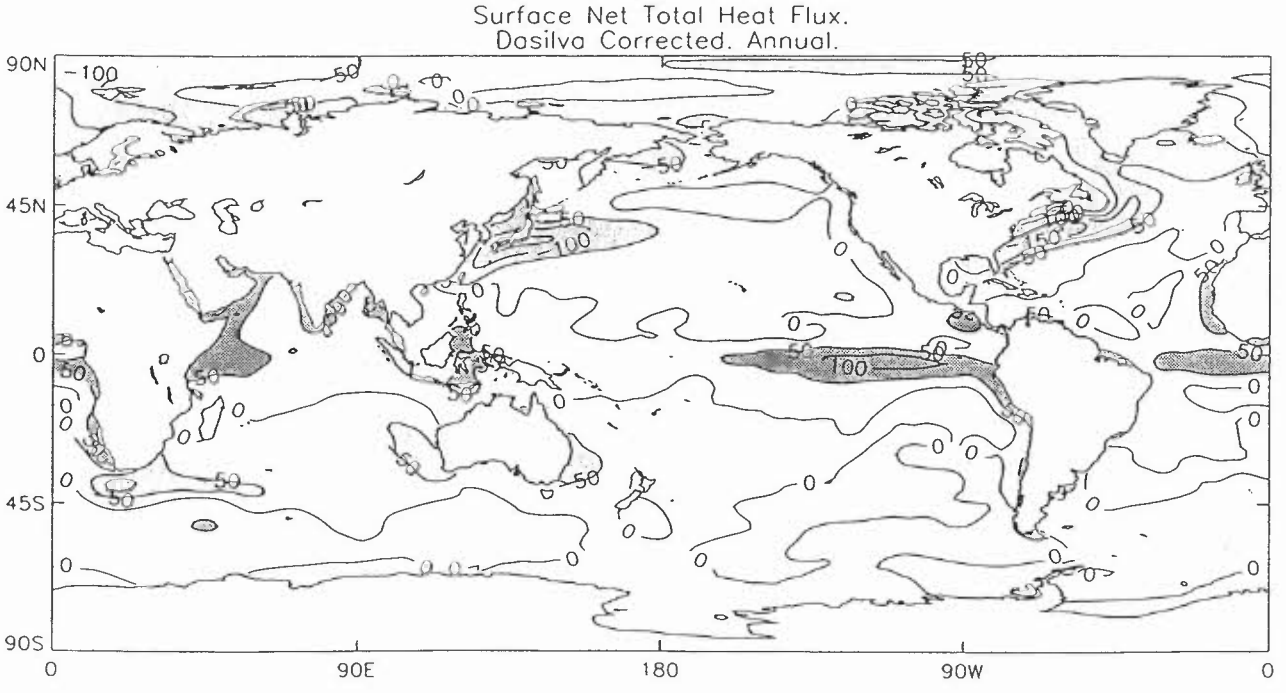

Fig.13 (a) Ten year annual mean of the net surface heat flux from the AMIP simulation with the HadAM3 model (contour interval is 50Wm^{-2}).
(b) Climatological surface heat flux from DS (contour interval is 50Wm^{-2}).

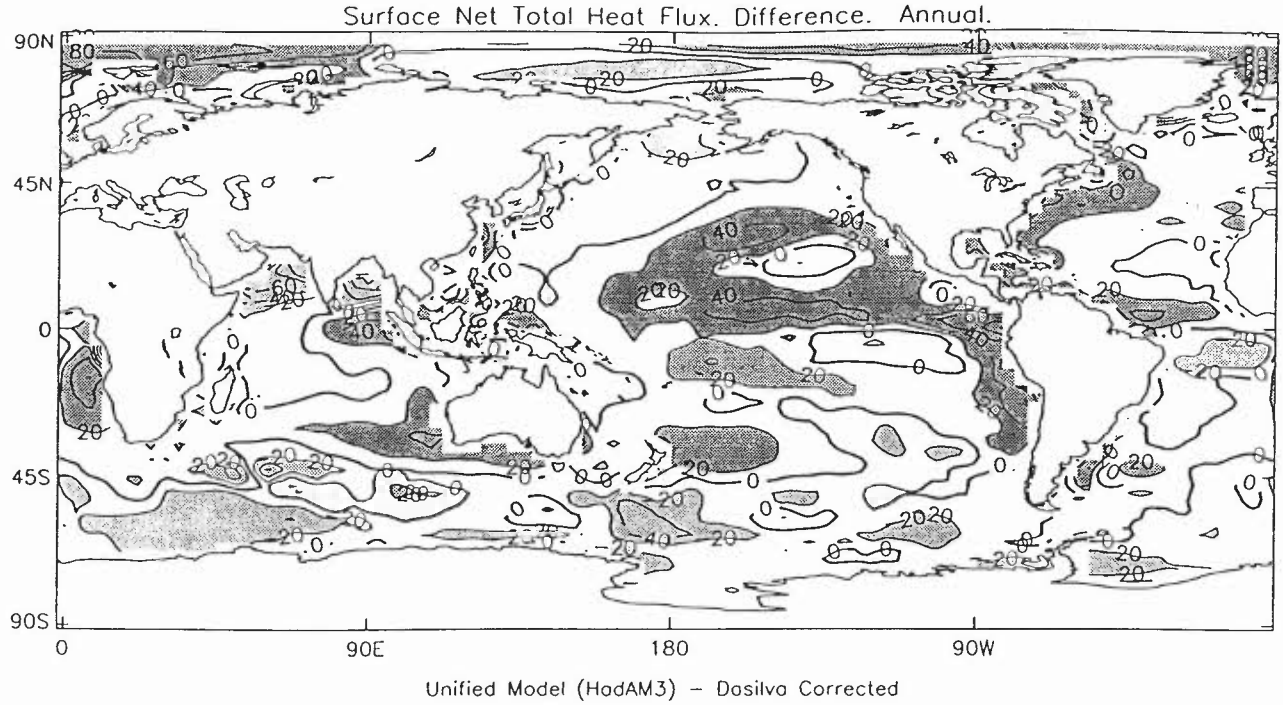

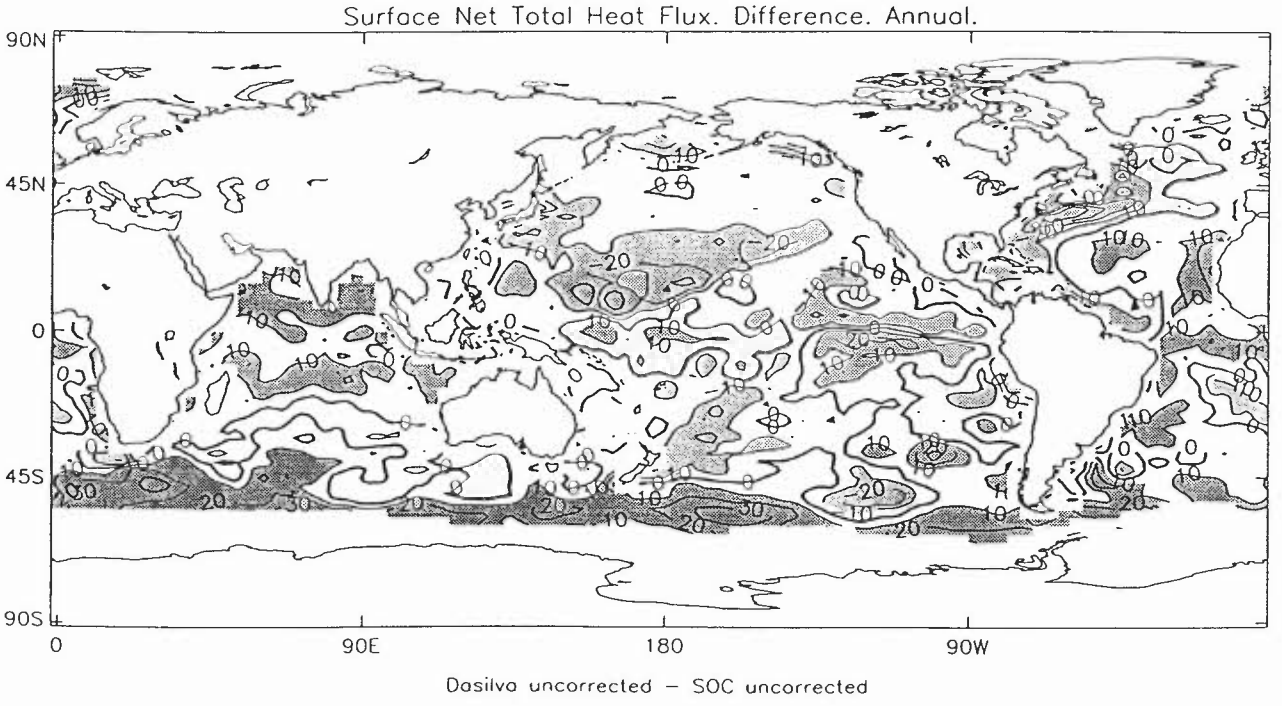

Fig.13 (c) Difference of model minus DS net surface heat flux (contour interval is $20Wm^{-2}$).

(d) Difference between the DS and Josey et al (1996) uncorrected climatologies of net surface heat flux (contour interval is $10Wm^{-2}$).

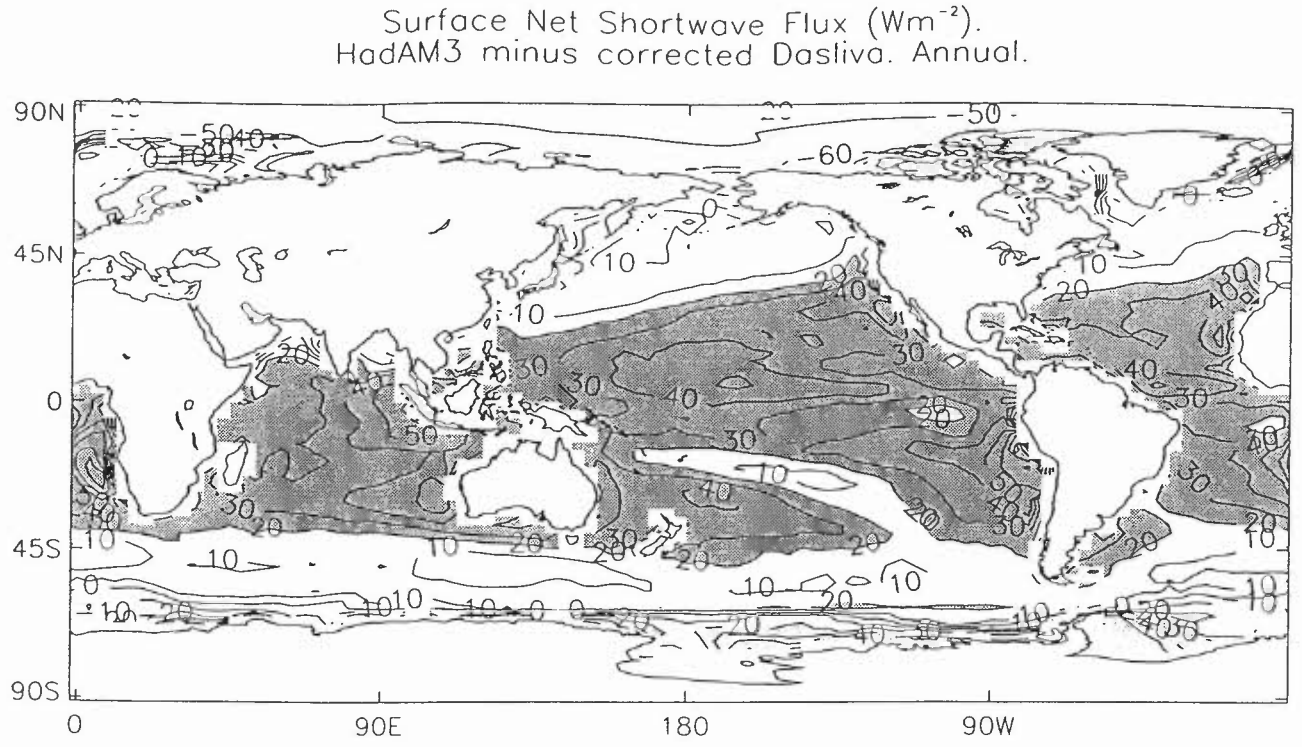

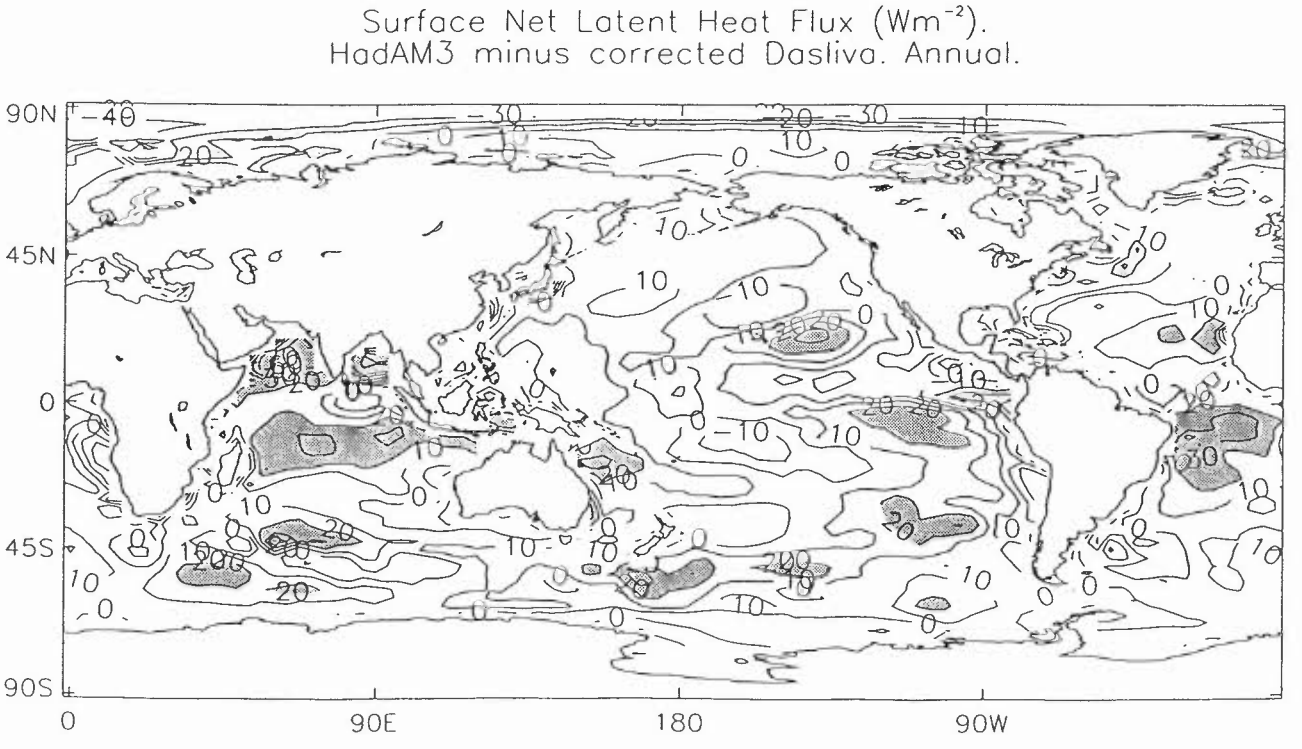

Fig. 14 (a) Difference between the ten year mean HadAM3 AMIP simulation of surface short wave flux and the DS climatology of the same quantity (the contour interval is 10Wm^{-2} and values differences greater than 20Wm^{-2} are shaded).
(b) As (14a) but for the surface latent heat flux.

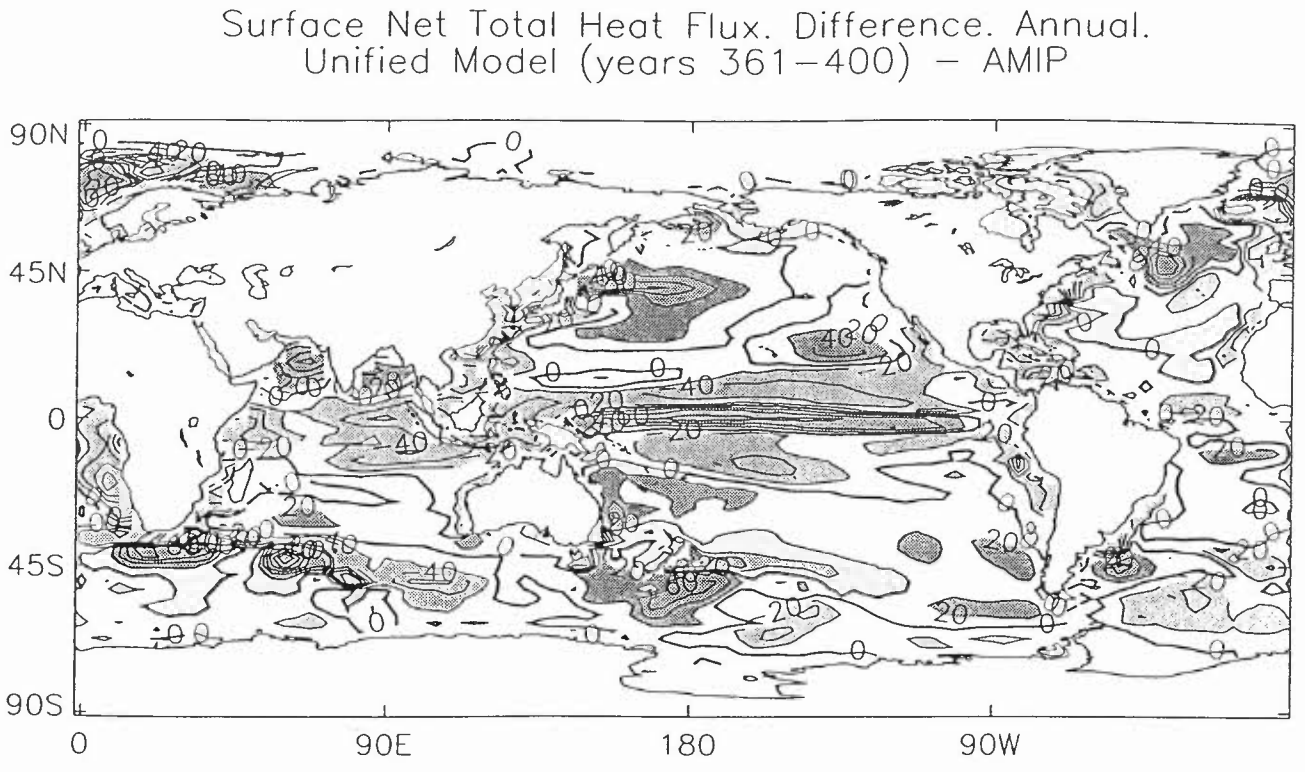

Fig.15 Difference between the HadCM3 coupled model (year 361-400) and AMIP simulation net surface heat flux (contour interval is $20Wm^{-2}$ and differences greater than $20Wm^{-2}$ are shaded).

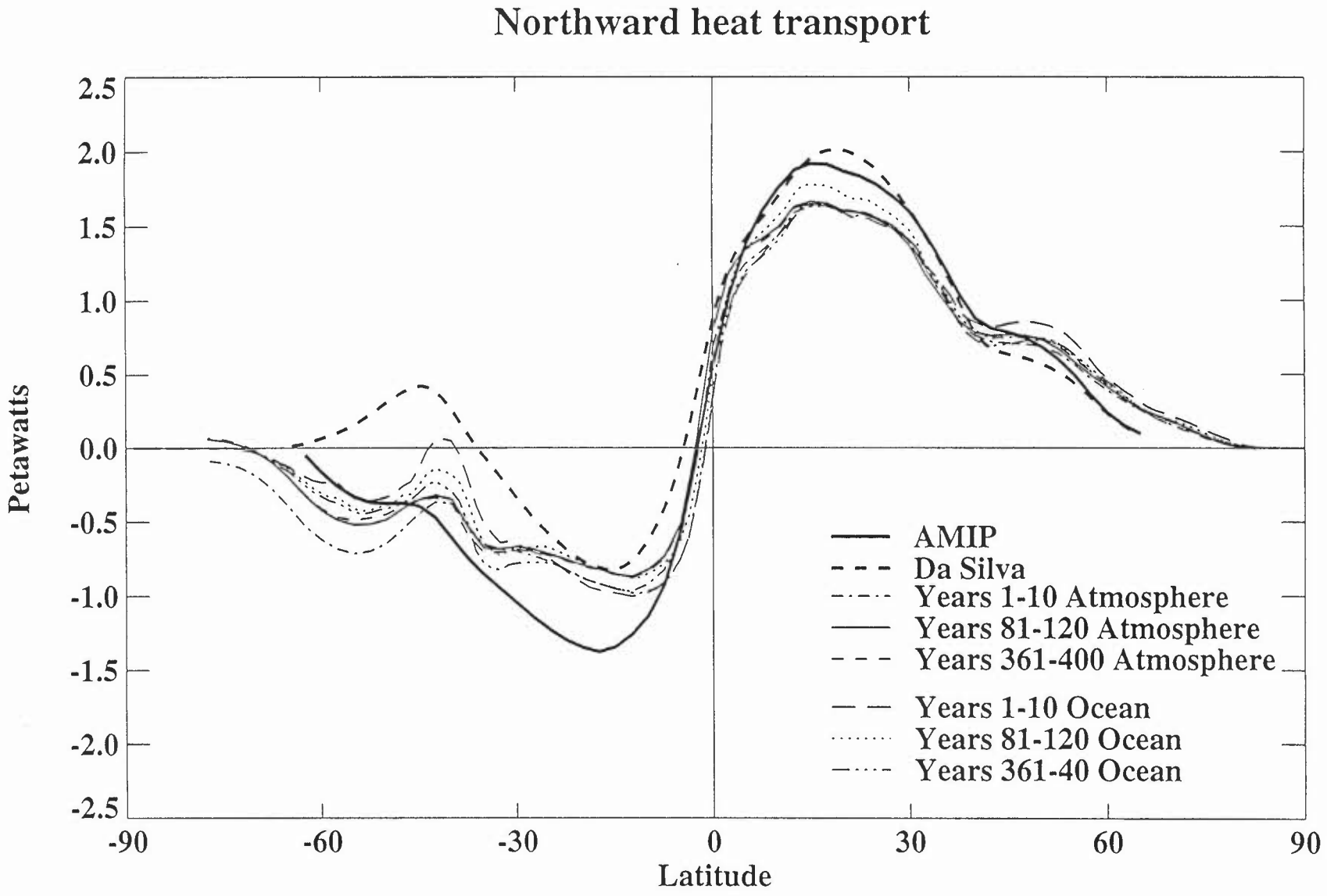

Fig.16 HadCM3 poleward heat transport (PW) as a function of latitude. See text for details.

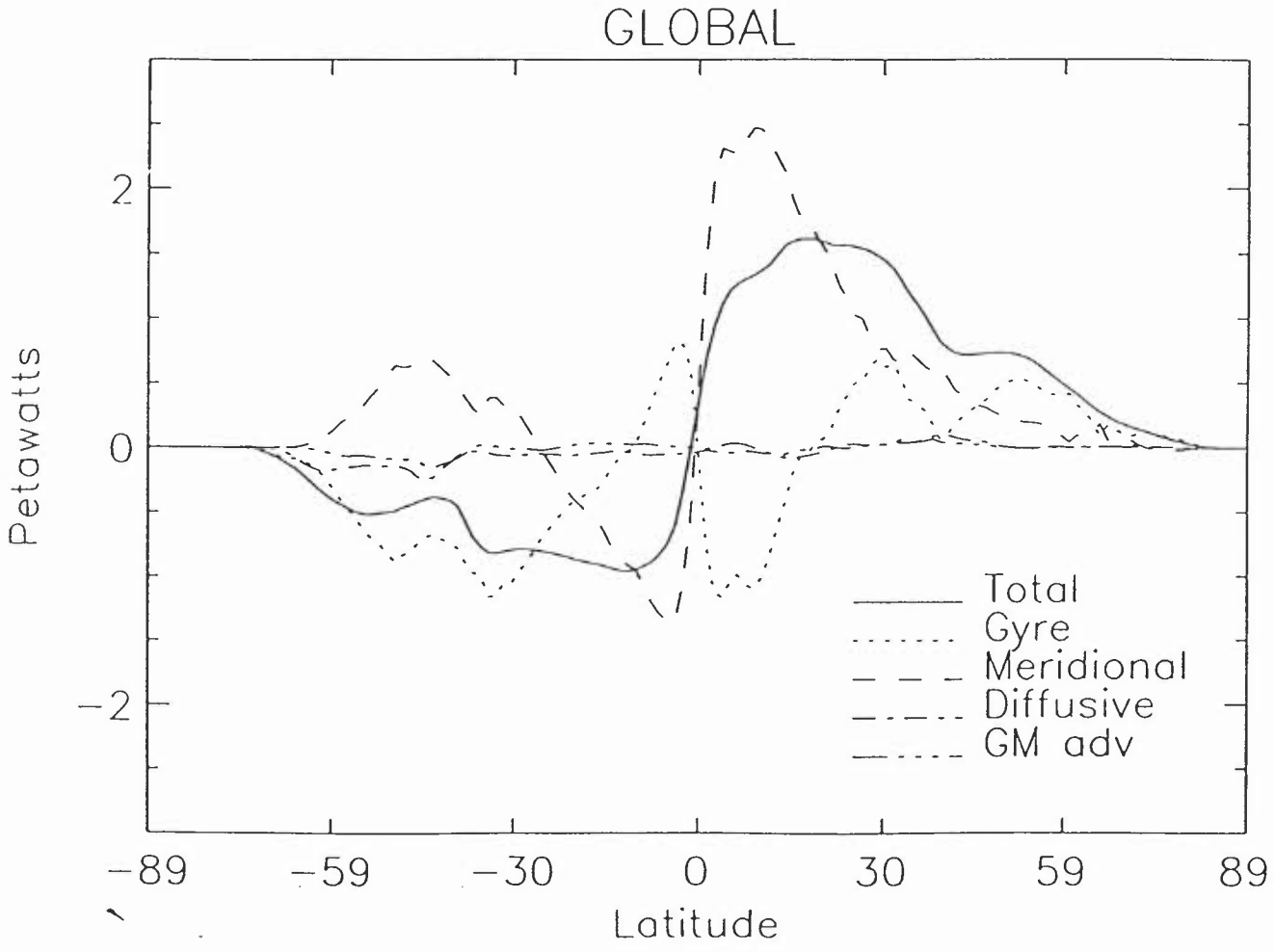

Fig. 17 HadCM3 component contributions of the poleward heat transport (years 361-400) as a function of latitude (PW).

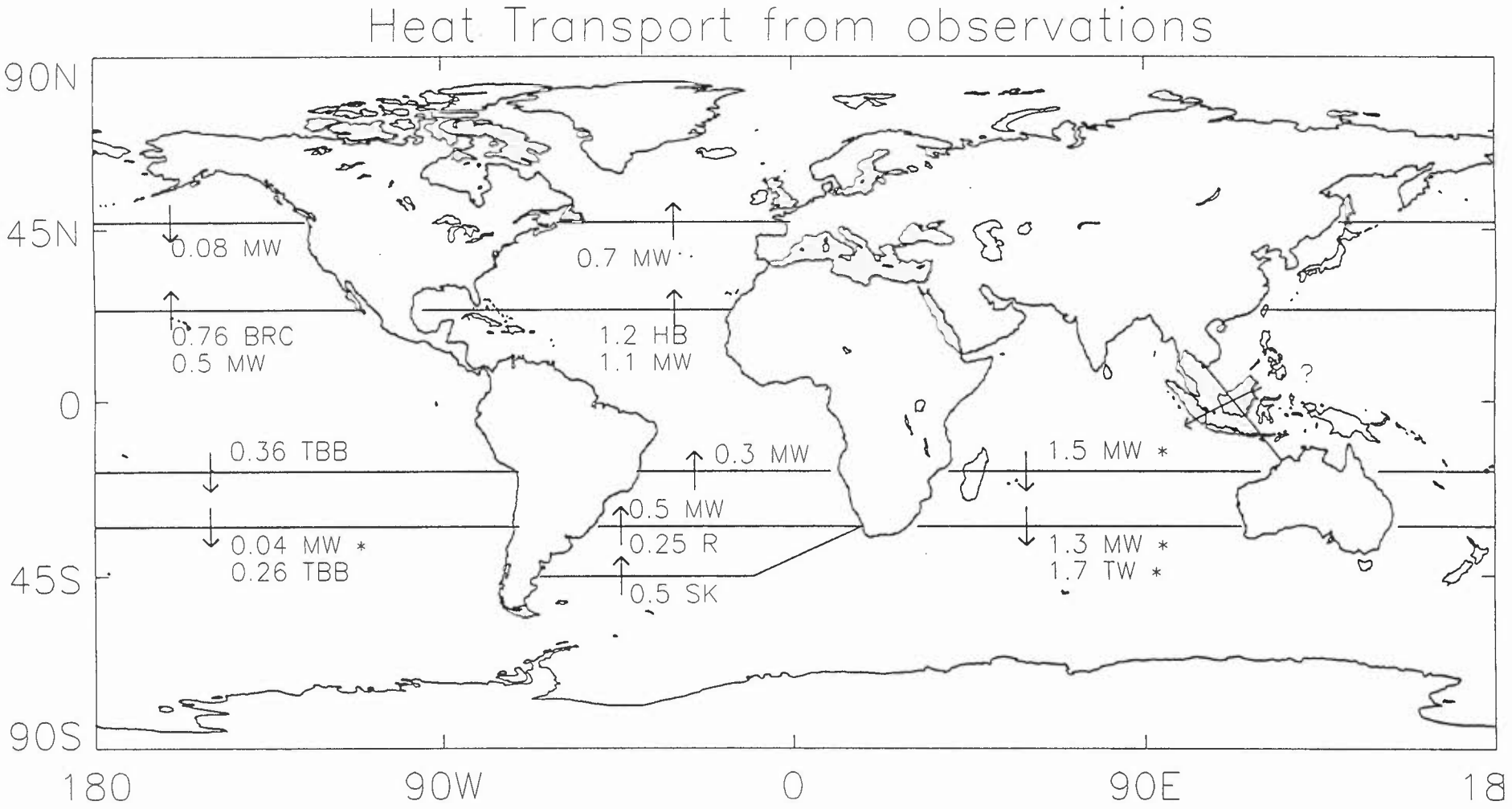

Fig.18 Direct ocean observational estimates of the meridional heat transport at marked altitudes. The authors for particular sections are indicated by initials.

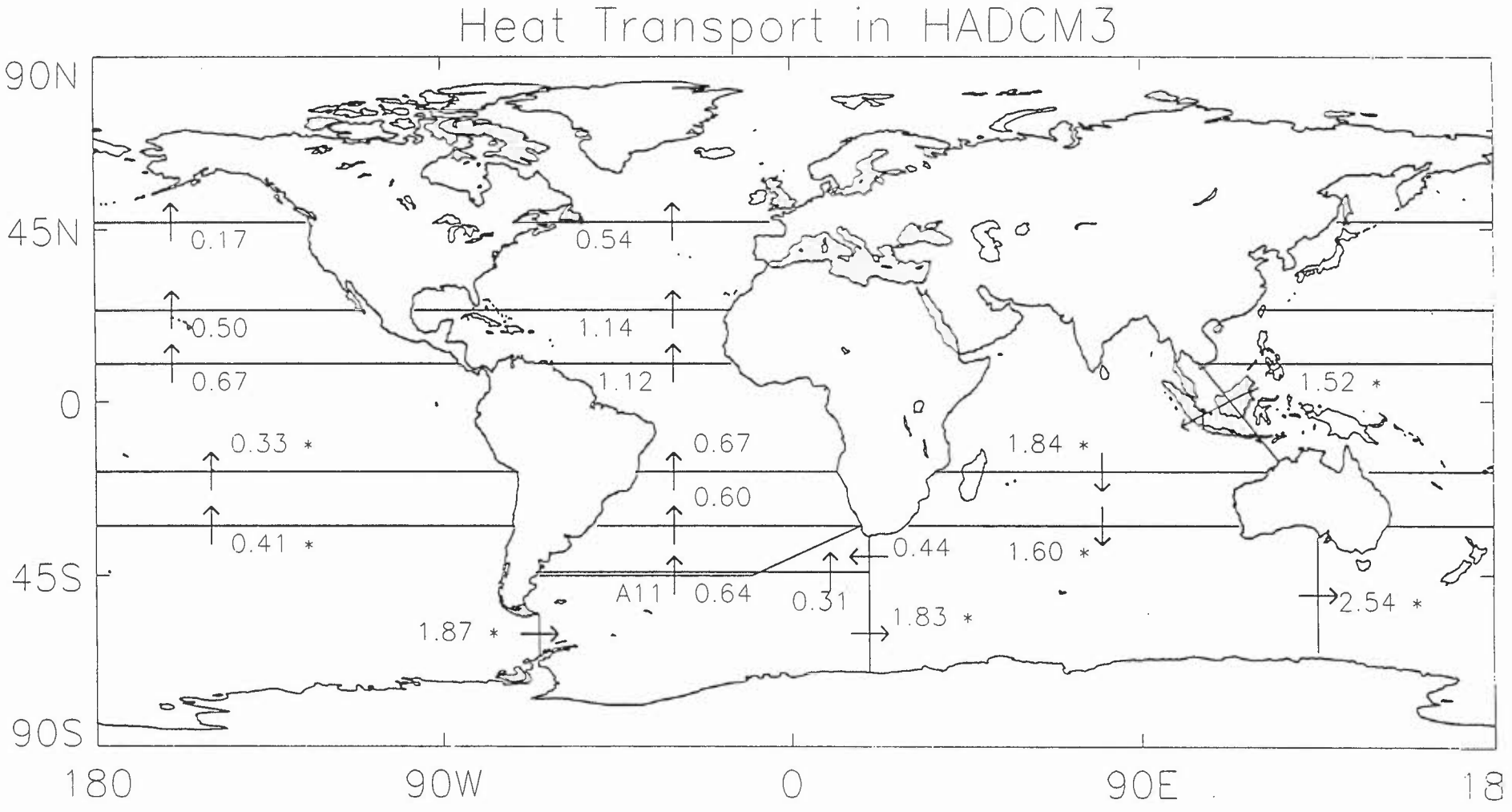

Fig.19 (a) As (18) but for the HadCM3 coupled model for years 81-120.

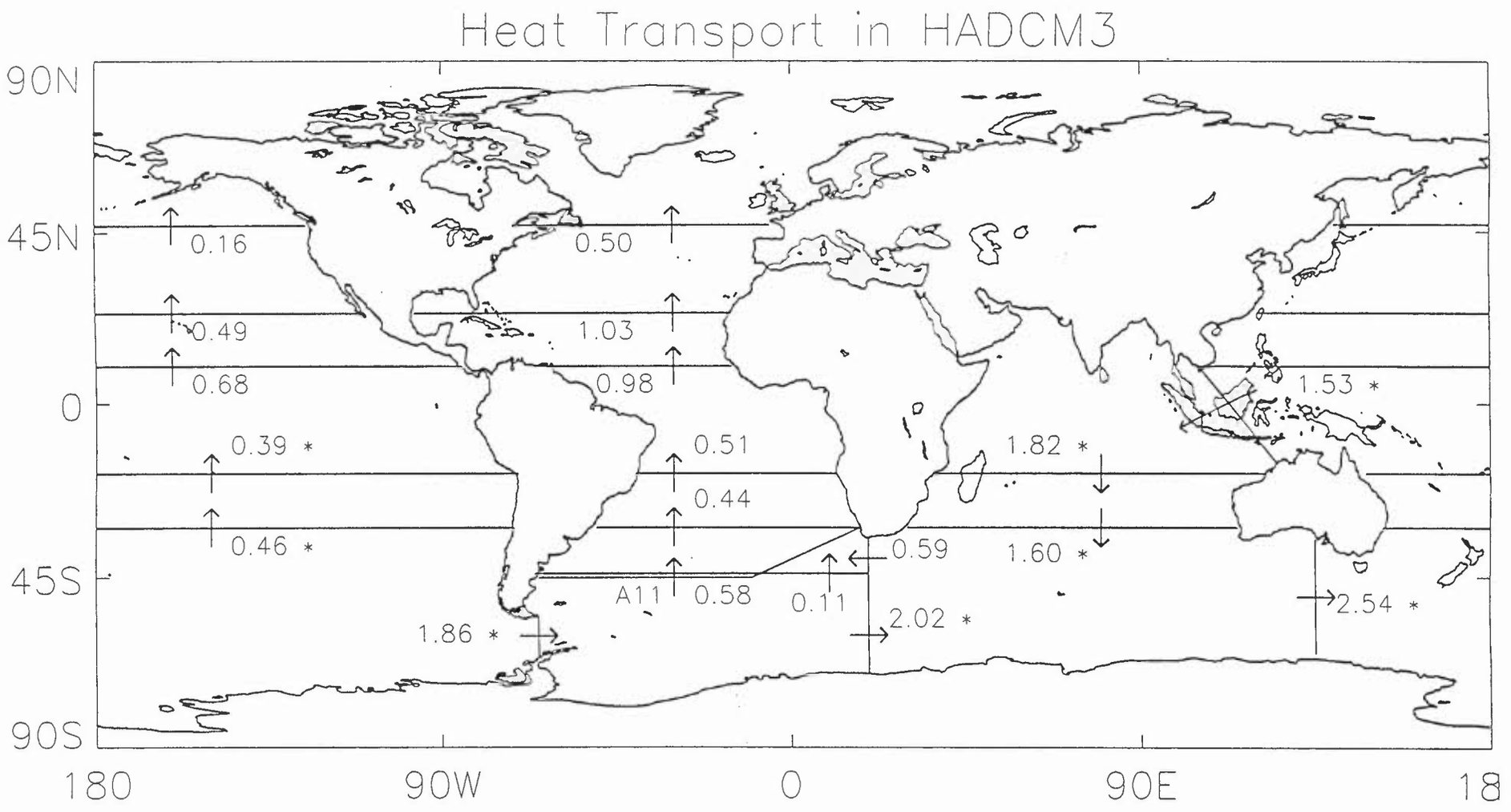

Fig.19 (b) As (18) but for the HadCM3 coupled model for years 361-400.
In both figs.19a and 19b some additional model sections are included.

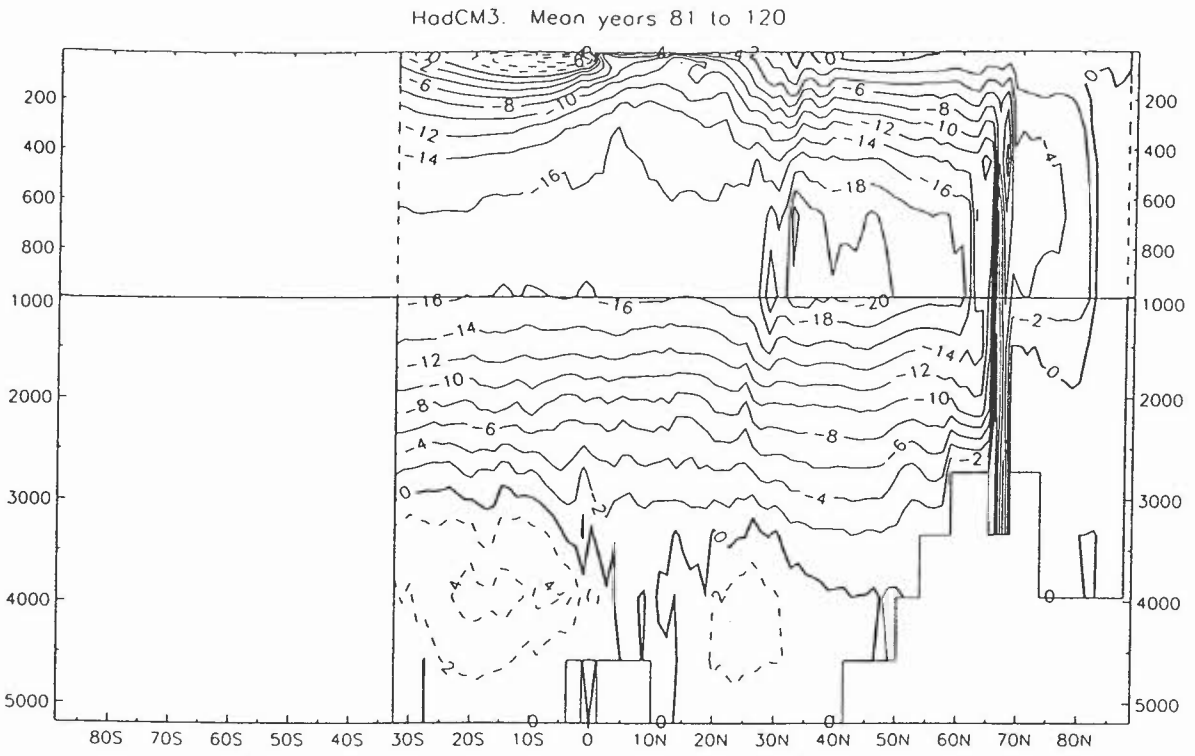

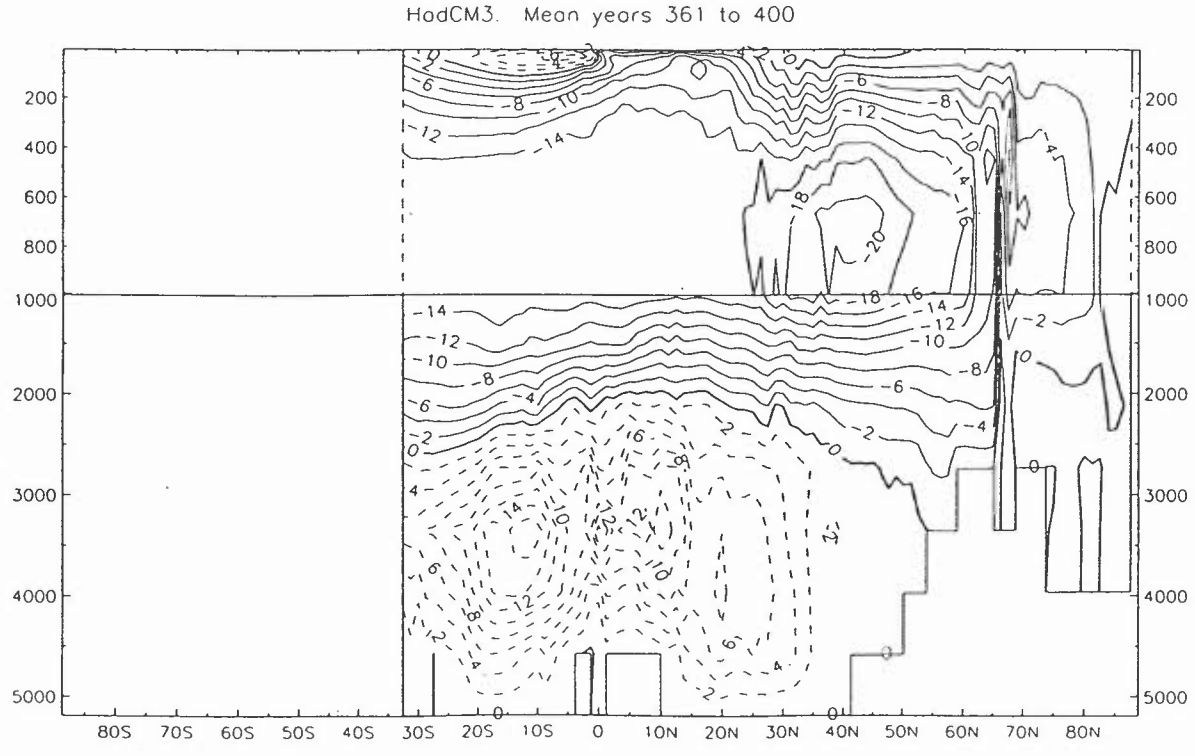

Fig.20 (a) North Atlantic overturning stream function (Sv) for years 81-120 of the HadCM3 coupled model.
(b) As (20a) but for years 361-400.